cmgh
CELLULAR AND MOLECULAR GASTROENTEROLOGY AND HEPATOLOGY

ORIGINAL RESEARCH

TAK1 Is a Novel Target in Hepatocellular Carcinoma and Contributes to Sorafenib Resistance

Shunjie Xia,[1,2,3,4,a] Lin Ji,[1,2,3,4,a] Liye Tao,[1,2,3,4,a] Yu Pan,[1,2,3,4] Zhongjie Lin,[1,2,3,4] Zhe Wan,[1,2,3,4] Haoqi Pan,[1,2,3,4] Jie Zhao,[1,2,3,4] Liuxin Cai,[1,2,3,4] Junjie Xu,[1,2,3,4] and Xiujun Cai[1,2,3,4]

[1]Key Laboratory of Laparoscopic Technology of Zhejiang Province, Department of General Surgery, Sir Run-Run Shaw Hospital, Zhejiang University School of Medicine, Hangzhou, China; [2]Zhejiang Minimal Invasive Diagnosis and Treatment Technology Research Center of Severe Hepatobiliary Disease, Zhejiang Research and Development Engineering Laboratory of Minimally Invasive Technology and Equipment, Hangzhou, China; [3]Zhejiang University Cancer Center, Hangzhou, China; and [4]Liangzhu Laboratory, Zhejiang University Medical Center, Hangzhou, China

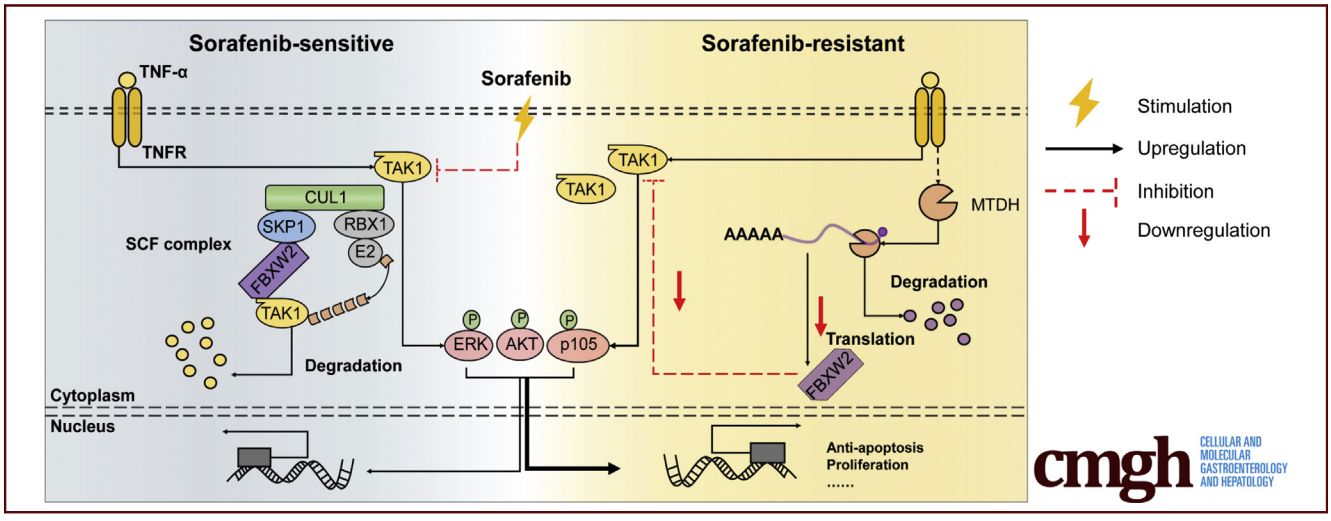

SUMMARY

The study unravels the clinical significance of TAK1 in HCC and sorafenib resistance. We identified a novel E3 ubiquitin ligase, FBXW2, targeting TAK1 for degradation, and MTDH contributes to TAK1 up-regulation through binding to FBXW2 mRNA and accelerates its degradation.

BACKGROUND & AIMS: Identifying novel and actionable targets in hepatocellular carcinoma (HCC) remains an unmet medical need. TAK1 was originally identified as a transforming growth factor-β–activated kinase and was further proved to phosphorylate and activate numerous downstream targets and promote cancer progression. However, the role of TAK1 in developed HCC progression and targeted therapy resistance is poorly understood.

METHODS: The expression of TAK1 or MTDH in HCC cell lines, tumor tissues, and sorafenib-resistant models was analyzed by in silico analysis, quantitative real-time polymerase chain reaction, Western blotting, and immunohistochemistry. In vivo and in vitro experiments were introduced to examine the function of TAK1 or MTDH in HCC and sorafenib resistance using small interfering RNA and pharmacologic inhibitors in combination with or without sorafenib. Co-immunoprecipitation and RNA immunoprecipitation were carried out to determine the binding between TAK1 and FBXW2 or between MTDH and FBXW2 mRNA. Protein half-life and in vitro ubiquitination experiment was performed to validate whether FBXW2 regulates TAK1 degradation.

RESULTS: Our findings unraveled the clinical significance of TAK1 in promoting HCC and sorafenib resistance. We identified a novel E3 ubiquitin ligase, FBXW2, targeting TAK1 for K48-linked polyubiquitylation and subsequent degradation. We also found that MTDH contributes to TAK1 up-regulation in HCC and sorafenib resistance through binding to FBXW2 mRNA and accelerates its degradation. Moreover, combination of TAK1 inhibitor and sorafenib suppressed the growth of sorafenib-resistant HCCLM3 xenograft in mouse models.

CONCLUSIONS: These results revealed novel mechanism underlying TAK1 protein degradation and highlighted the therapeutic value of targeting TAK1 in suppressing HCC and overcoming sorafenib resistance. *(Cell Mol Gastroenterol Hepatol 2021;12:1121–1143; https://doi.org/10.1016/j.jcmgh.2021.04.016)*

Keywords: Hepatocellular Carcinoma; Sorafenib; Drug Resistance; TAK1; Ubiquitin-Mediated Proteolysis.

Liver cancer is among the most commonly diagnosed cancers and the leading cause of cancer deaths. Hepatocellular carcinoma (HCC) comprises 75%–85% of liver cancer cases.[1] HCC is of great tumor heterogeneity, which is the major cause of tumor progression and treatment failures and could be the result of diverse mutations that have been identified by studies through multiomics approaches.[2] Sorafenib is the first targeted drug but provides limited improvement in patient survival because of the low frequency of sorafenib-targeting mutations and the early occurrence of secondary drug resistance in HCC patients.[3] As we previously reviewed, the underlying mechanisms of sorafenib resistance involve various cellular processes, complex regulatory signaling network, genetic and epigenetic regulations, and tumor microenvironment.[4] On the basis of these researches, numerous drugs including small molecule agonists or inhibitors, epigenetic, metabolic, or microenvironmental modulators, stemness inhibitors, oxidative stress inducers, and even nucleic acid therapies were being explored in combination with sorafenib to improve HCC patient outcomes.[4–6] However, none of them had been applied in clinical use. Hence, identifying targets especially those with multiple signals convergence or divergence to overcome sorafenib resistance is of great clinical significance.

Transforming growth factor-β–activated kinase 1 (TAK1, also known as MAP3K7) can be activated by a diverse set of intracellular and extracellular stressors and is known to regulate nuclear factor kappa B (NF-κB), transforming growth factor-β, and mitogen-activated protein kinase signaling pathways. Accumulating studies demonstrated that TAK1 mediates pro-survival activities, tumor progression, and chemoresistance in cancers.[7] However, as a hub of cellular homeostasis, the activity of TAK1 is context-dependent and cancer type-dependent, which is mainly attributed to the dual effect of TAK1-mediated NF-κB and transforming growth factor-β signaling in cancers.[8] The role of TAK1 in liver is diverse. Early studies presented that TAK1 deletion in hepatocytes caused severe cell death, compensatory proliferation, hepatic inflammation, liver fibrosis, and early-onset of hepatocarcinogenesis.[9,10] However, TAK1 deletion is rarely found in HCC patients according to The Cancer Genome Atlas (TCGA) database. Moreover, recent studies also proved that TAK1 was associated with poor survival of HCC patients and promoted hepatic steatosis, epithelial-mesenchymal transition (EMT) phenotypes, drug resistance, and cancer metastasis.[11–13] These studies indicated that TAK1 might exert pro-survival function in transformed malignant hepatocytes. In this context, the role of TAK1 in HCC progression and therapy resistance requires further elucidation.

TAK1 activity is regulated by its binding partners TAB1 and TAB2/TAB3 and relies on post-translational modifications including ubiquitination and phosphorylation.[14] Several E3 ligases, deubiquitinating enzymes, and phosphatases had been previously identified mediating K63-linked polyubiquitylation or deubiquitylation and dephosphorylation of TAK1, leading to TAK1 activation or inactivation.[7,11,15,16] However, the E3 candidates targeting TAK1 for K48-linked polyubiquitylation and degradation are largely unknown. MTDH has already been proved to be a master regulator in several crucial aspects of tumor progression, including transformation, evasion of apoptosis, invasion, metastasis, and chemoresistance. TAK1 has a large overlap with MTDH in terms of downstream pathways and biological functions.[17,18] However, whether MTDH and TAK1 regulate with each other remains unknown, and their roles in sorafenib resistance have not been well-studied.

Here we demonstrated that both MTDH and TAK1 contribute to HCC progression and sorafenib resistance, with the combination of the in vitro and in vivo studies and clinical data analysis from HCC patients. We identified FBXW2 as a novel E3 ubiquitin ligase targeting TAK1 for K48-linked polyubiquitination and degradation, and MTDH functions as an upstream effector of TAK1 at post-translational level through binding to FBXW2 mRNA and promoting its degradation. Our results highlighted the key roles and the molecular mechanisms of MTDH/TAK1 axis in HCC and sorafenib resistance, thus providing novel targets for clinical intervention.

Results

TAK1 Expression Is Up-Regulated in Developed HCC

We first analyzed the mutation status and expression of TAK1 in silico using TCGA database, Gene Expression Omnibus (GEO) dataset (GSE14520), and our own dataset (Sir Run-Run Shaw Hospital [SRRSH]). We observed that TAK1 deletion is rarely found in HCC patients (6/366), not to mention missense mutation (3/366) with unknown function in TCGA dataset (Figure 1*A*). But mRNA expression of TAK1 was significantly elevated in human HCC tissues as compared with non-tumorous livers (Figure 1*B*). Moreover, analysis of GSE6764 dataset revealed that TAK1 expression was already up-regulated in very early HCC and tended to increase with HCC progression (Figure 1*C*). We also observed ranging TAK1 protein level among different HCC

[a]Authors share co-first authorship.

Abbreviations used in this paper: **CHX, cycloheximide; DAPI, 4′,6-diamidino-2-phenylindole; DFS, disease-free survival; DMSO, dimethyl sulfoxide; EMT, epithelial-mesenchymal transition; GEO, Gene Expression Omnibus; GSEA, gene set enrichment analysis; HCC, hepatocellular carcinoma; IC50, half maximal inhibitory concentration; IHC, immunohistochemistry; IP, immunoprecipitation; NAFLD, nonalcoholic fatty liver disease; NASH, nonalcoholic steatohepatitis; NF-κB, nuclear factor kappa B; OXO, 5z-7-oxozeaenol; qPCR, quantitative polymerase chain reaction; RIP, RNA immunoprecipitation; RT, real-time; siRNA, small interfering RNA; SR, sorafenib-resistant; SRRSH, Sir Run Run Shaw Hospital; TAK1, transforming growth factor-β–activated kinase 1; TCGA, The Cancer Genome Atlas; TNF-α, tumor necrosis factor-alpha.**

Most current article

2352-345X
https://doi.org/10.1016/j.jcmgh.2021.04.016

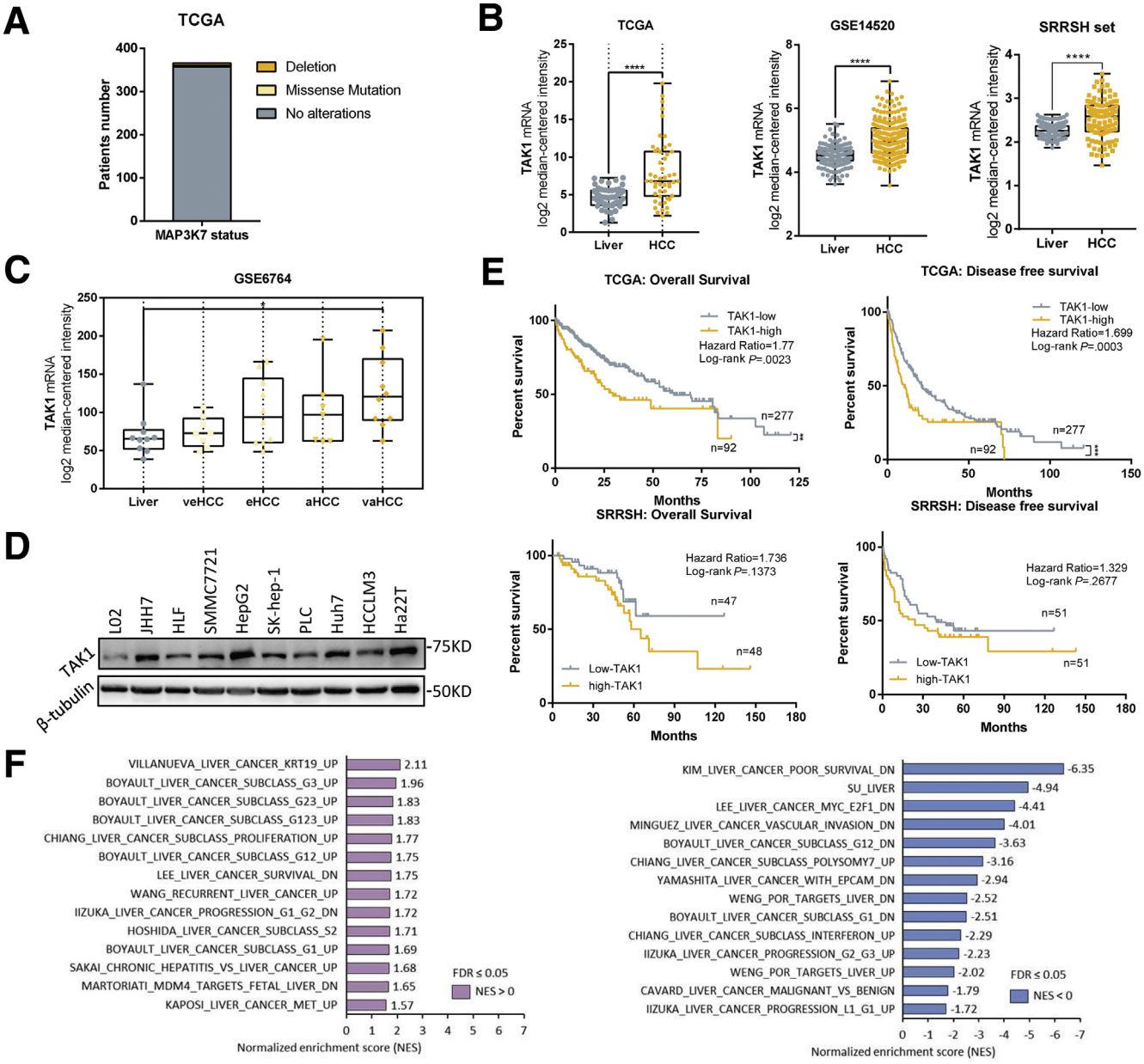

Figure 1. TAK1 expression in HCC. (*A*) MAP3K7 (encoding TAK1 protein) mutation status in TCGA database; (*B*) mRNA expression of TAK1 in human HCC tissues as compared with non-tumorous livers from TCGA, GSE14520, and SRRSH datasets. (*C*) mRNA expression of TAK1 in different stages of HCC from GSE6764 dataset. (*D*) Protein level of TAK1 among different HCC cell lines compared with normal liver cell lines (L02 and Chang). (*E*) Kaplan-Meier survival curves of patients with low or high TAK1 mRNA expression based on TCGA and SRRSH datasets. Significance was determined using Kaplan-Meier analysis. Survival analysis was performed using log-rank test. (*F*) Gene sets associated with TAK1 expression using TCGA data and GSEA analysis.

cell lines, almost all of which exhibited higher TAK1 expression than that in normal liver cells (Figure 1*D*). Survival analysis of TCGA dataset showed that TAK1 expression was negatively correlated with overall survival (OS) and disease-free survival (DFS) of HCC patients (Figure 1*E*). Moreover, SRRSH dataset analysis revealed similar results (Figure 1*E*). To address the role of TAK1 in HCC patients, we carried out gene set enrichment analysis (GSEA) using TCGA data and revealed that high TAK1 expression was positively correlated with a series of up-regulated gene sets in HCC and was negatively correlated with those down-regulated in HCC (Figure 1*F*). Taken together, these data suggested that although artificial TAK1 deletion leads to HCC initially, TAK1 functions as a tumor promoter in developed HCC and is a potential prognostic marker of HCC patients.

TAK1 Suppression Inhibits Clonogenicity, Proliferation, and Oncogenic Signaling in HCC

To better address the function of TAK1 in HCC, we carried out experiments to determine the functional impact of

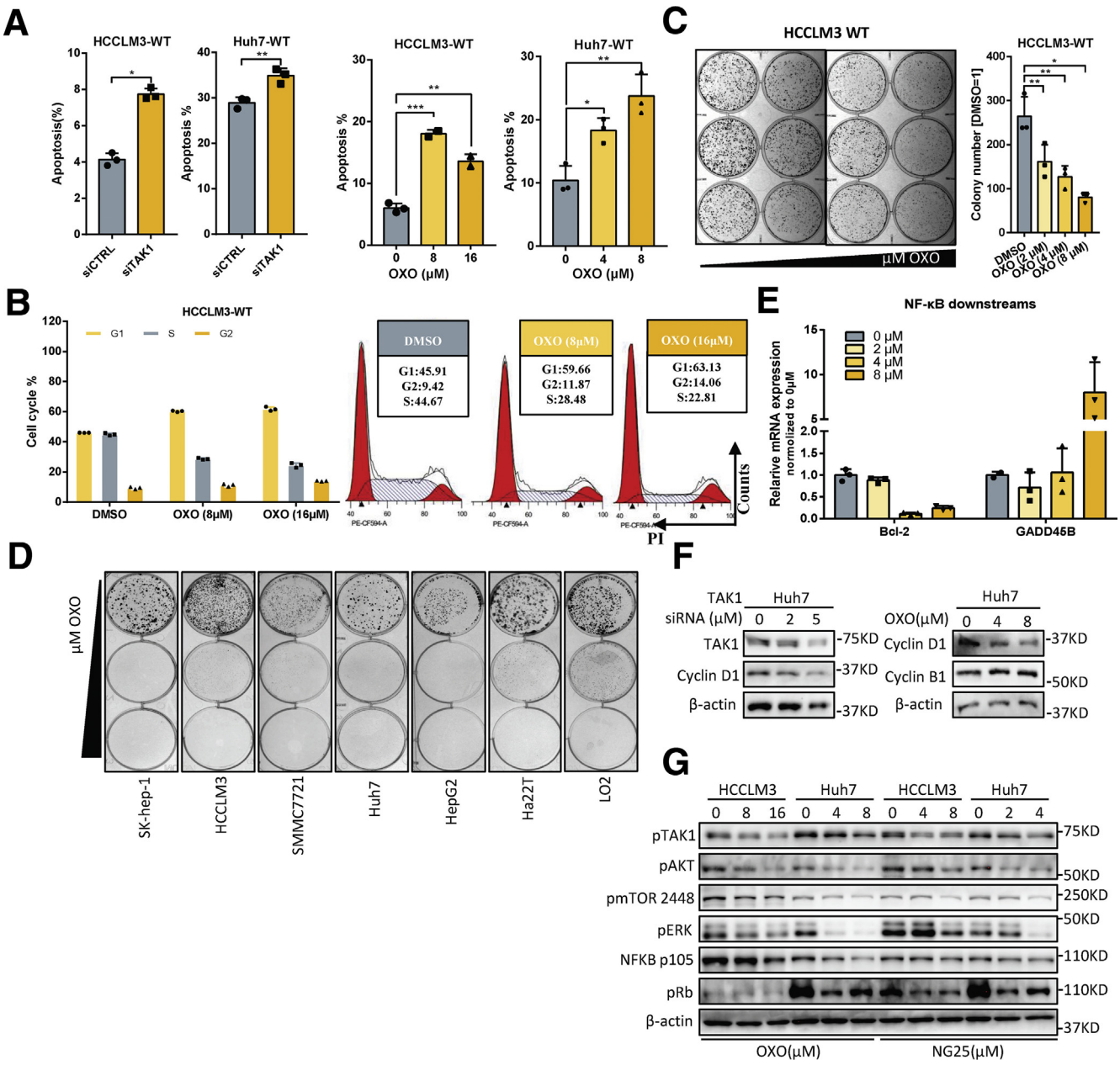

Figure 2. Function of TAK1 in HCC. (*A*) Proportion of annexin V-stained apoptotic cells analyzed by flow cytometry in Huh7 or HCCLM3 cells transfected with TAK1 siRNA or OXO treatment, a TAK1 inhibitor. Three biological repeats per group. (*B*) Cell cycle analysis and representative results of HCCLM3 cells using flow cytometry on OXO treatment. Three biological repeats per group. (*C*) Colony formation of HCCLM3 cells treated with different concentration of OXO. Colony numbers were measured by Image J software. Three biological repeats per group. (*D*) Colony formation of different HCC cell lines on OXO treatment with different concentrations. (*E*) Real-time (RT) qPCR quantification of Bcl-2 and GADD45β mRNA in HCCLM3 cells treated with OXO or not. (*F* and *G*) Western blotting analysis of TAK1 downstream proteins levels on genetic knockdown or pharmacologic inhibition of TAK1 in Huh7 and HCCLM3 cells.

TAK1 in Huh7 and HCCLM3 cell lines. Genetic knockdown of TAK1 by specific small interfering RNA (siRNA) and pharmacologic inhibition of phospho-TAK1 by 5z-7-oxozeaenol (OXO)[19] both strongly induced apoptosis in these 2 cell lines, with increased annexin V–stained apoptotic cells and accumulated floating cell fragments (Figure 2*A*, Figure 3*A*–*C*). In addition, TAK1 suppression also caused cell cycle arrest in G1 phase and inhibited clonogenicity of HCC cells (Figure 2*B* and *C*). Moreover, TAK1 suppression inhibited cell proliferation in most HCC cell lines (Figure 2*D*). TAK1 was known to boost NF-κB phosphorylation and its transcriptional activity,[12] which mediates the transcription of numerous pro-survival and anti-apoptosis signals in HCC.[20] Therefore, we tested the mRNA expression of NF-κB targets through quantitative polymerase chain reaction (qPCR), and the results showed lower expression of

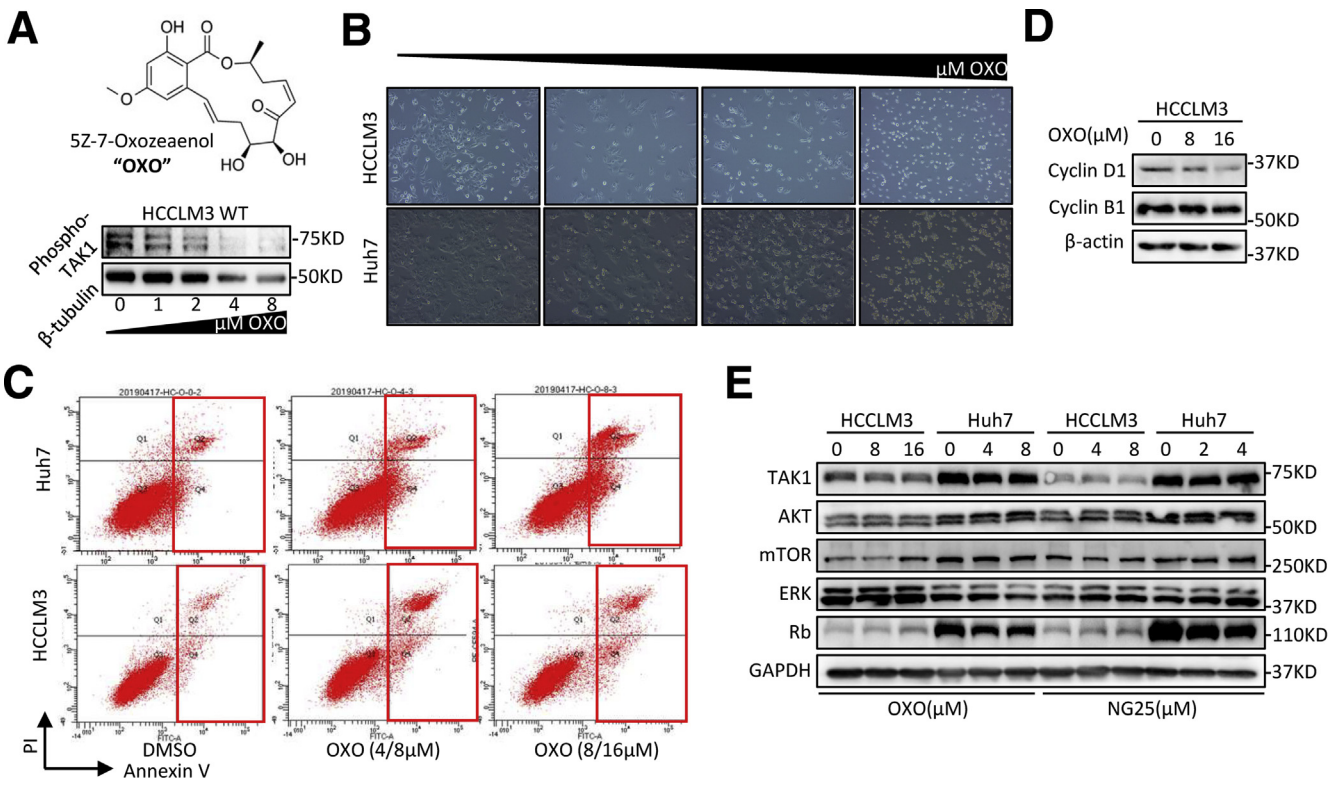

Figure 3. Supplementary data for TAK1 inhibition in HCC cell lines. (*A*) Western blotting analysis of phosphorylated TAK1 protein at ser439 site in HCCLM3 cells on treatment of OXO. (*B*) Representative images of HCCLM3 treated with OXO of increasing concentrations. (*C*) Representative results of flow cytometry analysis of HCCLM3 and Huh7 cells treated with OXO or not. (*D*) Western blotting analysis of cyclin D1 and cyclin B1 in HCCLM3 on OXO treatment. (*E*) Western blotting analysis of total TAK1 downstream proteins in HCCLM3 and Huh7 on OXO or NG-25 treatment.

Bcl-2, an anti-apoptosis regulator, and higher expression of GADD45B, a DNA damage inducer, on OXO treatment (Figure 2*E*). TAK1 activates multiple oncogenic signals, which were known to be critical players in HCC tumorigenesis. Indeed, OXO treatment or TAK1 knockdown significantly reduced the protein expression of phosphorylated ERK, phosphorylated AKT, phosphorylated mTOR, phosphorylated Rb, and cyclin D1 but not cyclin B1, whereas total protein levels of above genes were not altered (Figure 2*F* and *G*, Figure 3*D* and *E*). Altogether, TAK1 suppression induced cell cycle arrest and cell apoptosis in HCC cells and inhibited clonogenicity, proliferation, and oncogenic signaling in vitro, indicating TAK1 as a potential target for developed HCC.

TAK1 Expression Can Be Reduced by Targeted Drugs and Is Retained in Sorafenib-Resistant Cell Lines

To unravel the role of TAK1 in sorafenib resistance, we established stable sorafenib-resistant (SR) models of normal HCC cell lines (Huh7, SK-hep-1, HepG2, and HCCLM3), following the instructions in previous study.[6,21] The SR was determined by the half maximal inhibitory concentration (IC50) shift toward a higher concentration in all the resistant cell lines compared with their parental cell lines (Figure 4*A*, Figure 5*A*). The colony formation assays also showed that SR cells are more proliferative under sorafenib treatment (Figure 5*B*).

Both primary and second drug resistance are mainly attributed to tumor heterogeneity.[22] In many tumor entities including HCC, therapy-induced evolving is achieved through epithelial-to-mesenchymal transition (EMT) and cancer stemness acquisition.[23–25] Therefore, we first characterized the mesenchymal state and stemness features in SR cell line models. As expected, we observed profound morphologic changes in SR cells transforming into spindle-like shape under an electron microscope (Figure 5*B*), indicating that SR cells were undergoing EMT process, which was one of the well-known underlying mechanisms of SR.[26] The EMT status in SR cells was further characterized by loss of ZO1 and gain of mesenchymal markers such as N-cadherin, although the expression of another epithelial marker E-cadherin was not consistently changed among 4 SR cell lines (Figure 4*C*). Unlike other studies,[21] the SR cells we build tend to cluster together rather than being separated from each other, especially under sorafenib treatment, and this might be attributed to the retention of E-cadherin to maintain cell-to-cell contacts (Figure 4*D*). These features might also be explained by the existence of intermediate EMT states and multifunction of E-cadherin according to recent advances in research.[27,28] EMT-related transcriptional factors are key regulators of EMT process and could also promote HCC progression.[29] We further checked the

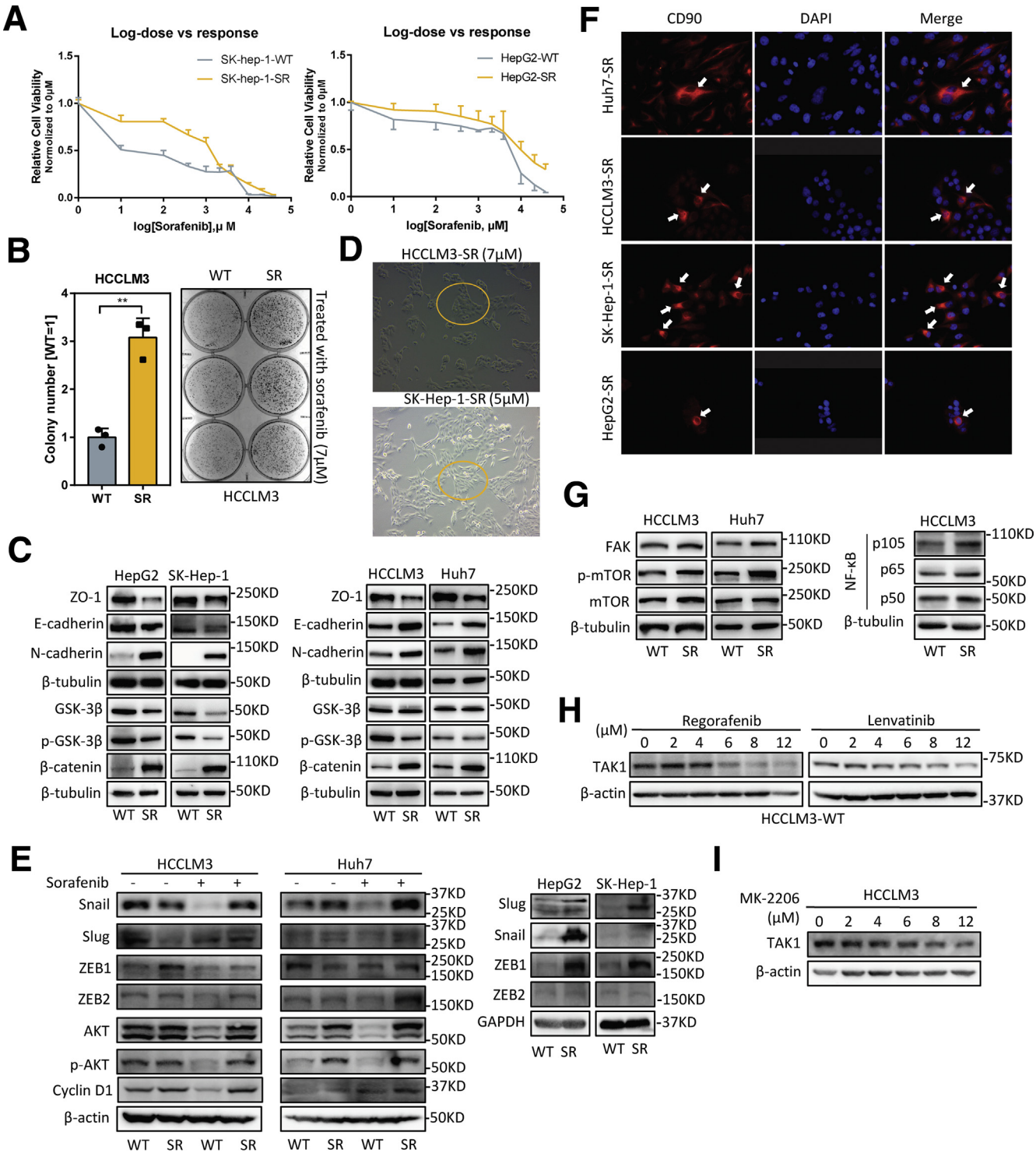

Figure 4. Features of SR cells. (*A*) Relative cell viability of SK-hep-1-SR and HepG2-SR cells on sorafenib treatment with increasing dosage compared with their parental cells. (*B*) Colony formation assay was performed in HCCLM3 wild-type (WT) and SR cells treated with sorafenib (7 μmol/L). Colony numbers were measured by Image J software. Three biological repeats per group. (*C*) Western blotting analysis of EMT-related markers and proteins in SR cells compared with their parental cells. (*D*) Representative images of HCCLM3-SR and SK-hep-1-SR cells treated with OXO of indicated concentrations. (*E*) Western blotting analysis of EMT-related transcriptional factors in SR cells compared with their parental cells on sorafenib treatment or not. (*F*) Representative images of CD90 staining in 4 SR cells. *Red*, CD90; *blue*, DAPI. (*G*) Western blotting analysis of TAK1 downstream proteins in SR cells compared with their parental cells. (*H* and *I*) Western blotting analysis of TAK1 protein in HCCLM3 cells on treatment of regorafenib, lenvatinib, or MK-2206.

expression of EMT- related transcriptional factors in SR cells compared with their parental cells on sorafenib treatment or not. The immunoblotting results showed that not all EMT-related transcriptional factors were changed accordingly, further indicating the heterogeneity at transcriptional level (Figure 4*E*). Because that gain of stemness improves

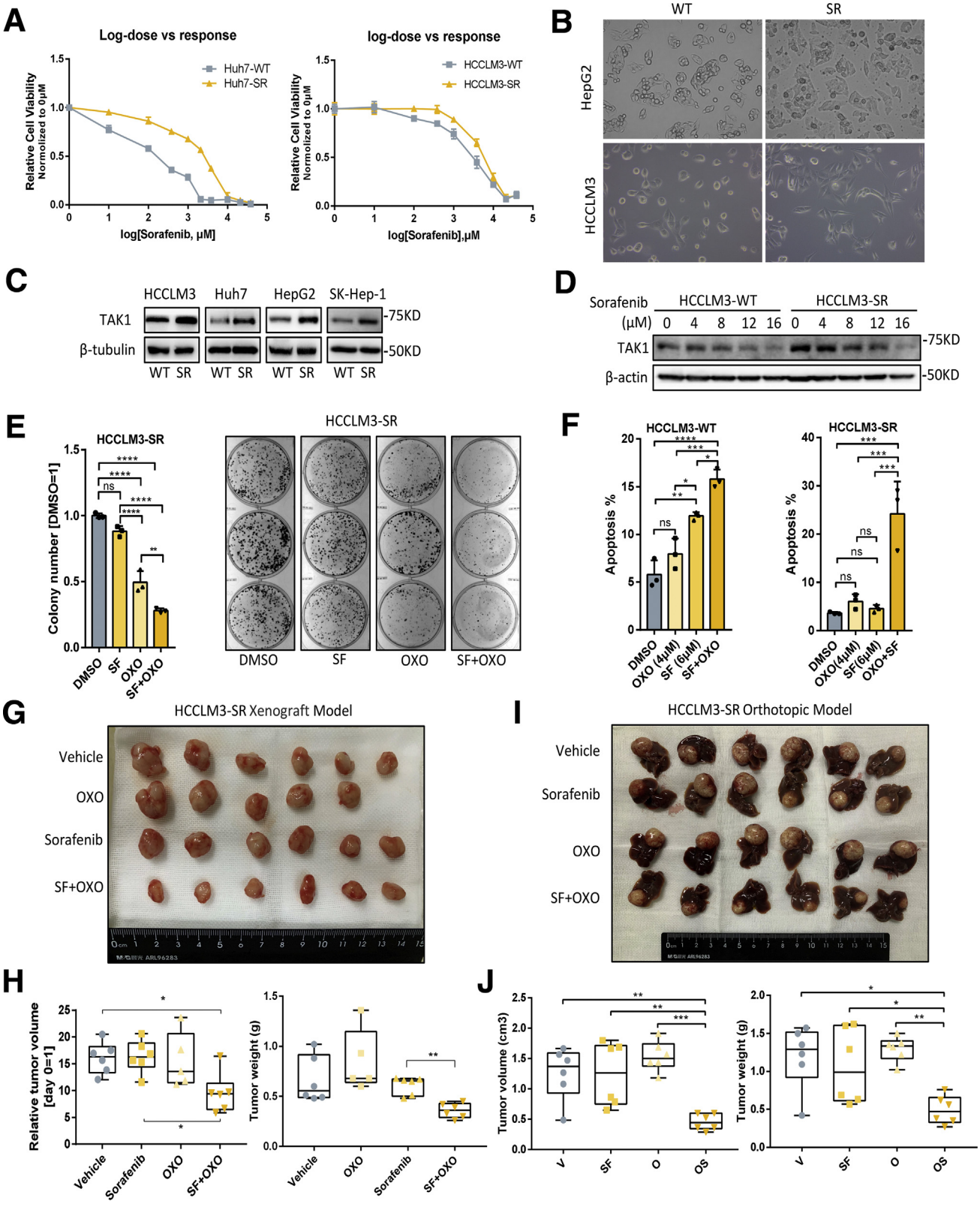

drug tolerance of normal tumor cells,[4] we examined the stem features of SR cells by CD90 staining, a stemness marker. Expectedly, CD90 positive SR cells were enriched in the center of normal SR cell clusters (Figure 4F), suggesting that some of SR cells acquired stemness traits and became the origin of sorafenib resistance. Oncogenic pathway activation and intracellular signaling compensation on drug treatment are important layers of HCC progression and sorafenib resistance.[30] Indeed, we revealed higher cyclin D1, p-AKT, FAK, p-mTOR, p105/p50, GSK-3β, and β-catenin expression in SR cells, indicating activation of MAPK, PI3K/AKT, NF-κB, and Wnt pathways in sorafenib resistance (Figure 4*C*, *E*, and *G*).

Next we detected the TAK1 expression in SR cells compared with the parental cells and observed significantly higher protein level of TAK1 in 4 SR cells (Figure 5*C*). Interestingly, on sorafenib treatment, the protein level of TAK1 decreases as the concentration increases in the parental HCC cells but decreases more slowly in SR cells (Figure 5*D*). Such TAK1 protein decreases could also be observed on regorafenib or lenvatinib treatment (Figure 4*H*). These suggested TAK1 is a direct or indirect target of targeted drugs. Sorafenib as well as other tyrosine kinase inhibitors are well-known to inhibit Ras/MEK/ERK and PI3K/Akt/mTOR pathways. In this context, we treated HCC cells with increasing concentration of AKT inhibitor, MK-2206. We found that AKT inhibitor decreased total protein of TAK1 as well, suggesting that sorafenib might regulate TAK1 level through AKT pathway (Figure 4*I*). We also believed that there are other factors involved. More importantly, the regulatory mechanism of TAK1 expression in SR cells on long-term sorafenib treatment might be totally different from short-term inhibitory effect on TAK1 expression.

Targeting TAK1 Overcomes Sorafenib Resistance in vitro and in vivo

High expression of TAK1 in SR cells also prompted us to explore whether targeting TAK1 pharmacologically or via genetic knockdown reverses sorafenib resistance of SR cells. Indeed, combination of sorafenib and OXO strongly inhibited its clonogenicity and proliferation compared with sorafenib or OXO treatment alone in SR cell models (Figure 5*E*). Flow cytometry assays showed that OXO or TAK1 knockdown in combination with sorafenib largely increased proportion of apoptotic HCC cells and re-sensitized SR cells to sorafenib-induced apoptosis, whereas both sorafenib and OXO alone induced apoptosis in parental cells (Figure 5*F*, Figure 6*A* and *B*). Particularly, we used an in vivo SR cells xenograft and tumor model to evaluate the combined anticancer effect of sorafenib and OXO by inoculating subcutaneously the HCCLM3-SR cells into the flank sides of nude mice, followed by treatment with vehicle control, OXO, or sorafenib alone or in combination. When nontoxic concentrations were used (Figure 6*D*), sorafenib or OXO alone did not suppress the tumor growth in vivo; however, significant suppression was observed in combination group in terms of tumor volumes, tumor weights, and Ki67-staining, as well as downstream oncogenic proteins (Figure 5*G* and *H*, Figure 6*D*–*F*). Because liver microenvironment has a crucial impact on sorafenib resistance, we also adopted in vivo orthotopic model, and consistent results were observed (Figure 5*I* and *J*, Figure 6*G* and *H*). Thus, TAK1 inhibitors sensitized HCC SR cells to sorafenib as tested in both in vitro cell culture and in vivo xenograft models.

FBXW2 E3 Ubiquitin Ligase Targets TAK1 for Ubiquitination and Degradation

To uncover the regulatory mechanism of TAK1 expression in SR cells, we first detected mRNA level of TAK1 and observed no consistently significant changes between SR cell lines and their parental cells (Figure 7*A*). Furthermore, chlorhexidine (CHX) assay indicated that the TAK1 protein degradation was retarded in SR cells (Figure 7*B*). K48-linked polyubiquitination and degradation of TAK1 are largely unknown. F-box proteins are components of SKP1–cullin 1–F-box protein E3 ligase complexes and have pivotal roles in multiple cellular activities.[31] However, none of F-box proteins have been proved to mediate TAK1 degradation. Following this lead, we first ectopically expressed a variety of F-box proteins including FBWX2 followed by immunoprecipitation (IP) pull-down and found in vitro interaction between FBXW2 and TAK1, although FBXW2 is not the only F-box protein that could bind to TAK1 but has the highest IP affinity of TAK1 (Figure 7*C*). F-box proteins bind short, defined degradation motifs in substrates.[32] Regarding FBXW2 of which the substrates remain largely unknown, the consensus degron sequences defined as TSXXXS were required for its binding to substrates such as SKP2.[33] Indeed, we also identified such motif

Figure 5. (***See previous page***). **TAK1 expression and function in sorafenib resistance.** (*A*) Relative cell viability of Huh7-SR and HCCLM3-SR cells on sorafenib treatment with increasing dosage compared with their parental cells. Relative cell viability was measured by cell counting kit 8 (CCK8) reagent and normalized to 0 μml/L. (*B*) Morphologic changes of Hepg2-SR and HCCLM3-SR cells compared with their parental cells. (*C*) Western blotting analysis of TAK1 protein level in 4 SR cells compared with their parental cells. (*D*) Western blotting analysis of TAK1 protein level in HCCLM3-SR cells compared with their parental cells in response to sorafenib treatment. (*E*) Colony formation assay was performed in HCCLM3-SR cells treated with sorafenib alone or in combination with OXO. Colony numbers were measured by Image J software. Three biological repeats per group. (*F*) Proportion of annexin V-stained apoptotic cells analyzed by flow cytometry in HCCLM3-SR or its parental cells treated with sorafenib alone or in combination with OXO. Three biological repeats per group. (*G*) Gross view of tumors from xenograft model treated with sorafenib alone or in combination with OXO. (*H*) Total volume or weight of tumor burden in mice treated with sorafenib alone or in combination with OXO from xenograft model. (*I*) Gross view of tumors attached with liver from orthotopic model treated with sorafenib alone or in combination with OXO. (*J*) Total volume or weight of tumor burden in mice treated with sorafenib alone or in combination with OXO from orthotopic model.

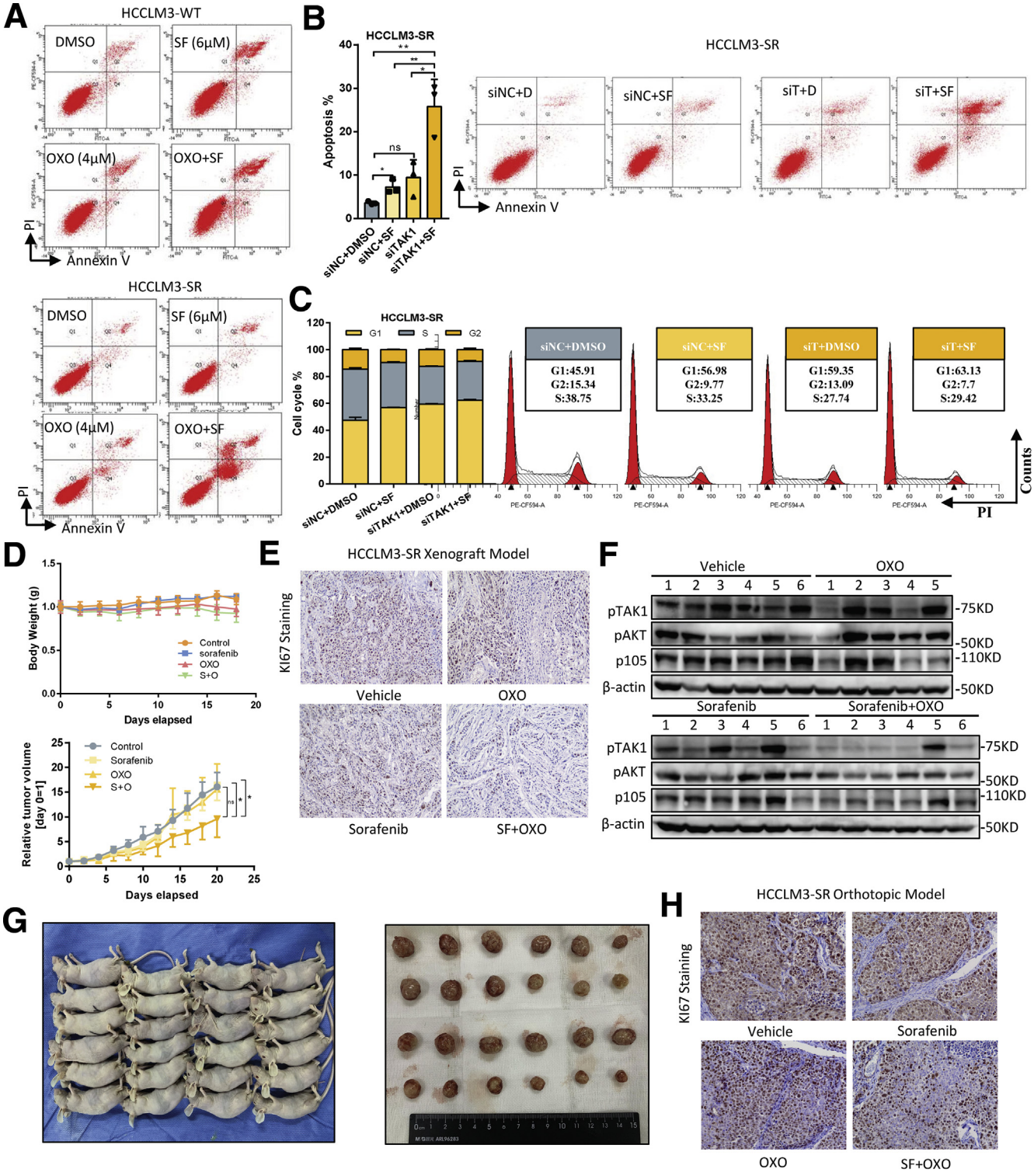

Figure 6. Supplementary data for TAK1 inhibition in combination with sorafenib in vivo. (*A*) Representative results of apoptosis analysis in HCCLM3-SR and its parental cells treated with sorafenib and OXO alone or in combination. (*B*) Proportion of annexin V-stained apoptotic cells analyzed by flow cytometry, and (*C*) cell cycle analysis and representative results of HCCLM3-SR cells transfected with TAK1 siRNA or scramble control. Three biological repeats per group. (*D*) Body weights of mice and total volume tumor burden in mice treated sorafenib alone or in combination with OXO in indicated time period. (*E*) Representative images of Ki67 staining in tumors from 4 groups. (*F*) Western blotting analysis of downstream proteins in tumors from mice treated with sorafenib and OXO alone or in combination. (*G*) Gross view of mice and tumors from orthotopic model. (*H*) Representative images of Ki67 staining of tumors from orthotopic model.

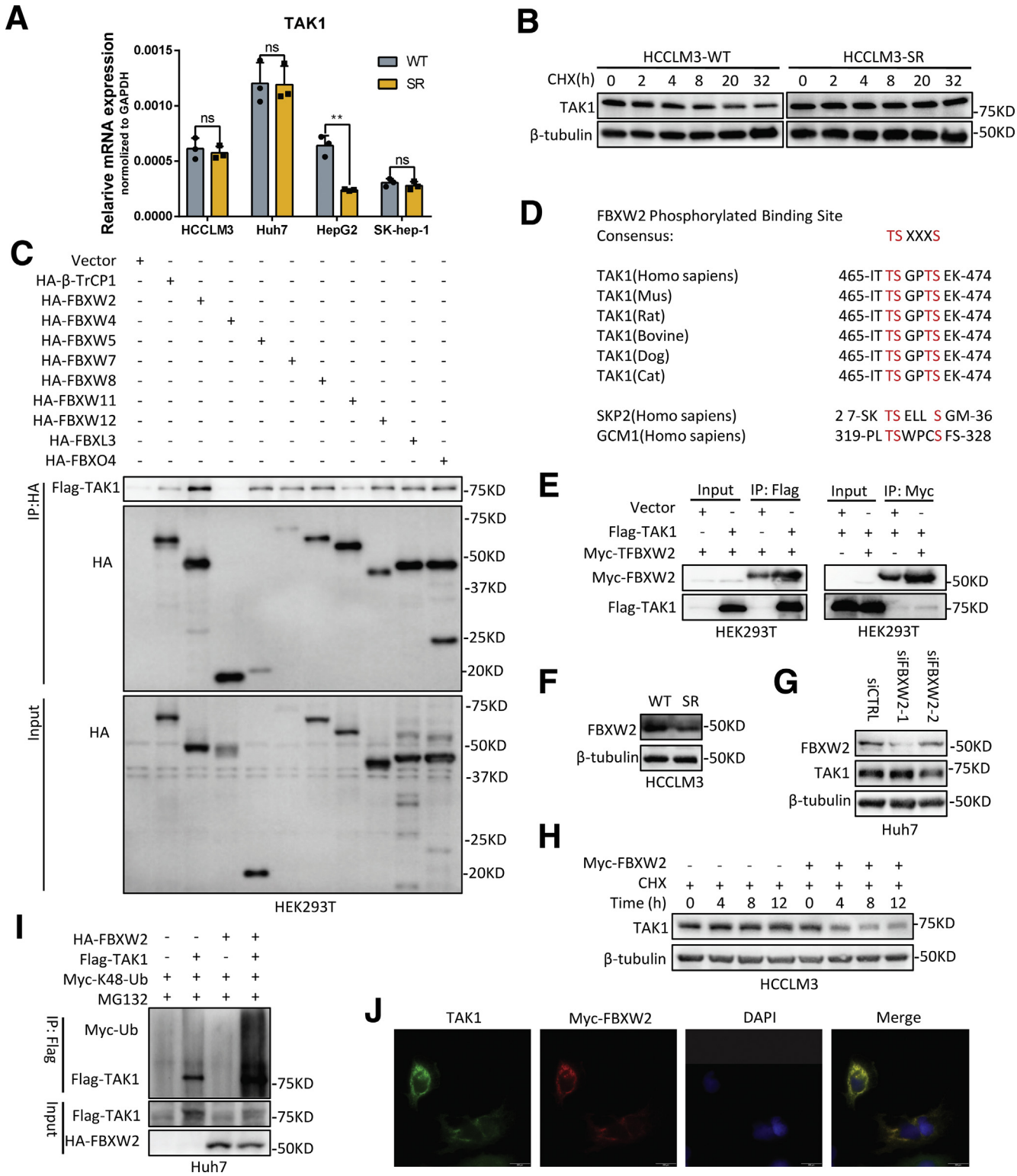

Figure 7. FBXW2 E3 ubiquitin ligase targets TAK1 for ubiquitination. (*A*) RT-qPCR quantification of TAK1 mRNA expression in 4 SR cells compared with their parental cells. (*B*) CHX assay was performed in HCCLM3-SR cells and their parental cells for indicated time periods, and TAK1 protein was measured by Western blotting analysis. (*C*) Immunoblotting analysis of HA and Flag-TAK1 in HA tag pull-down derived from HEK293T cells transfected with indicated constructs. (*D*) Evolutionary conservation of FBXW2 degron motif on TAK1. (*E*) HEK293 cells were transfected with indicated plasmids, followed by IP with anti-Flag or anti-Myc (*F*) Western blotting analysis of FBXW2 expression in HCCLM3-SR and its parental cells. (*H*) Half-life of TAK1 protein in HCCLM3 cells transfected with Myc-FBXW2 or vector plasmid as control. (*I*) Immunoblotting analysis of Myc-Ub in Flag tag pull-down and input derived from HEK293T cells transfected with indicated constructs. (*J*) Immunofluorescence analysis of TAK1 and Myc-FBXW2 location in Huh7 cells. *Green*, TAK1; *red*, Myc-FBXW2; *blue*, DAPI.

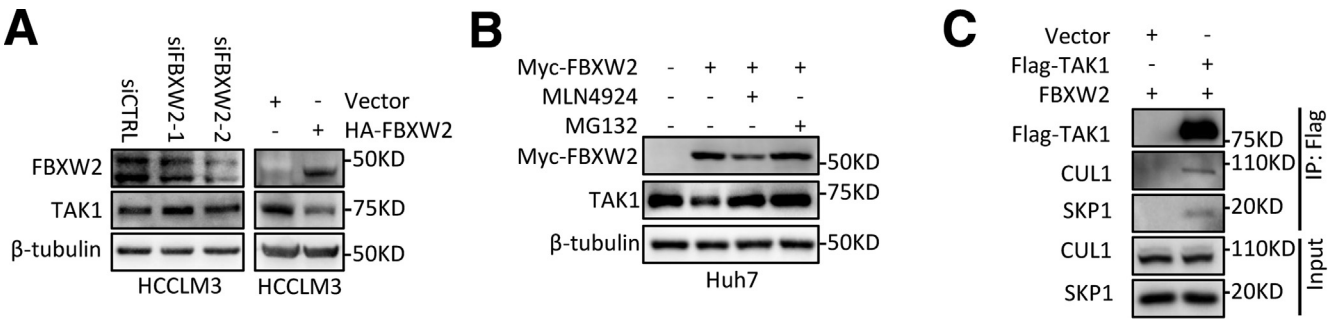

Figure 8. Supplementary data for TAK1 and FBXW2. (*A* and *B*) Western blotting analysis of TAK1 expression in HCCLM3 cells or Huh7 cells with FBXW2 knockdown or overexpression, treated with MG132 or MLN4924. (*C*) Immunoblotting analysis of CUL1 and SKP1 in Flag tag pull-down and input derived from HEK293T cells transfected with indicated constructs.

in TAK1, which is evolutionarily conserved (Figure 7*D*), suggesting TAK1 is a potential substrate of FBXW2. The binding of FBXW2 and TAK1 was then specifically confirmed by IP pull-down of Flag-TAK1 or Myc-FBXW2 (Figure 7*E*).

Notably, it was found that FBXW2 protein expression was down-regulated in SR cells compared with parental HCC cells, indicating that it might be responsible for retarded degradation of TAK1 in SR cells (Figure 7*F*). Hence, we assessed the effect of FBXW2 on TAK1 level. Indeed, FBXW2 knockdown increased the levels of total TAK1 protein, whereas FBXW2 overexpression reduced them, which could be reversed by MG132 or MLN4924, a NEDD8-activating enzyme inhibitor that inhibits the neddylation of the Cullin subunits of Cullin RING E3 ligases (Figure 7*G*, Figure 8*A* and *B*). These data together with the existence of SKP1 and CUL1 protein in TAK1 immunoprecipitants (Figure 8*C*) suggested that FBXW2 regulated TAK1 protein level through SKP1-CUL1-FBXW2 complex. Indeed, FBXW2 promoted TAK1 K48-linked polyubiquitylation and shortened its protein half-life (Figure 7*H* and *I*). Immunofluorescence analysis suggested that TAK1 and FBXW2 were co-localized in cytoplasm (Figure 7*J*). Taken together, we identified FBXW2 as a new E3 ubiquitin ligase targeting TAK1 for K48-linked polyubiquitylation and degradation.

MTDH Regulates TAK1 at Protein Level Through Promoting FBXW2 mRNA Degradation

The upstream regulators of TAK1 remain largely unknown, whereas its downstream effectors have been widely explored. As a master regulator of cell death, TAK1 is well-known to regulate NK-κB pathway. Tumor necrosis factor-alpha (TNF-α)/NF-κB pathway plays important role in the development of inflammation-driven HCC including viral hepatitis-related and nonalcoholic steatohepatitis (NASH)- or nonalcoholic fatty liver disease (NAFLD)-related HCC.[34] Recent study also indicated that TNF-α might serve as a predictor of sorafenib response in HCC patients.[35] Following this clue, it is quite possible that TAK1 upstream regulators might also regulate NF-κB signaling and contribute to drug resistance. We reviewed relative articles in PubMed and found that MTDH functions similarly with TAK1 in tumor progression and therapy resistance, activates common downstream pathways, and responds to similar intracellular or extracellular stimuli.[7,17] Moreover, GSEA analysis of defined gene sets revealed that MTDH was highly involved in RNA degradation and ubiquitin-mediated proteolysis (Figure 9*A*). In line with this, several researches had implied that MTDH acted as an RNA-binding protein.[36–38] Also illustrated was the decreased mRNAs that could bind to MTDH including a large amount of E2 and E3 ubiquitin ligases such as FBXW2 on a dual PI3K/mTOR inhibitor treatment.[36] This indicates that MTDH could accelerate the degradation of these mRNAs in response to drug stimuli. However, the role of MTDH in RNA stability or translation is not known. These findings suggested that MTDH might regulate TAK1 expression through inhibiting FBXW2 mediated TAK1 degradation. We first treated HCC cells with TNF-α. Results showed that TNF-α treatment increased MTDH and TAK1 protein expression but decreased FBXW2 protein level in a time course and in a dose-dependent manner (Figure 9*B*).

We then altered the MTDH levels to examine its effect on TAK1 level. MTDH knockdown significantly reduced TAK1 protein expression, whereas the mRNA levels of TAK1 were not consistent among 4 HCC cell lines (Figure 9*C* and *D*, Figure 10*A* and *B*), indicating that post-translational regulations were involved. Indeed, further mechanistic dissection demonstrated that MTDH knockdown could accelerate the protein degradation of TAK1 (Figure 9*E*). We thus detected the mRNA expression of those E2 and E3 ligases on MTDH knockdown and found that the decrease of MTDH expression increased their mRNA level (Figure 10*C*). Regarding FBXW2, MTDH knockdown also increased its protein level in HCC cells (Figure 9*F*).

Altogether, we hypothesized that MTDH regulates K48-linked polyubiquitination and degradation of TAK1 through down-regulating its E3 ubiquitin ligase FBXW2. We first used RNA-IP (RIP) and revealed much higher MTDH-bound FBXW2 mRNA compared with immunoglobulin G, suggesting the specific association of FBXW2 mRNA and MTDH (Figure 9*G*). Immunofluorescence and fluorescence in situ hybridization assay for MTDH protein and FBXW2 mRNA also showed that FBXW2 mRNA overlapped with those MTDH localized at cytoplasm (Figure 9*H*). Moreover,

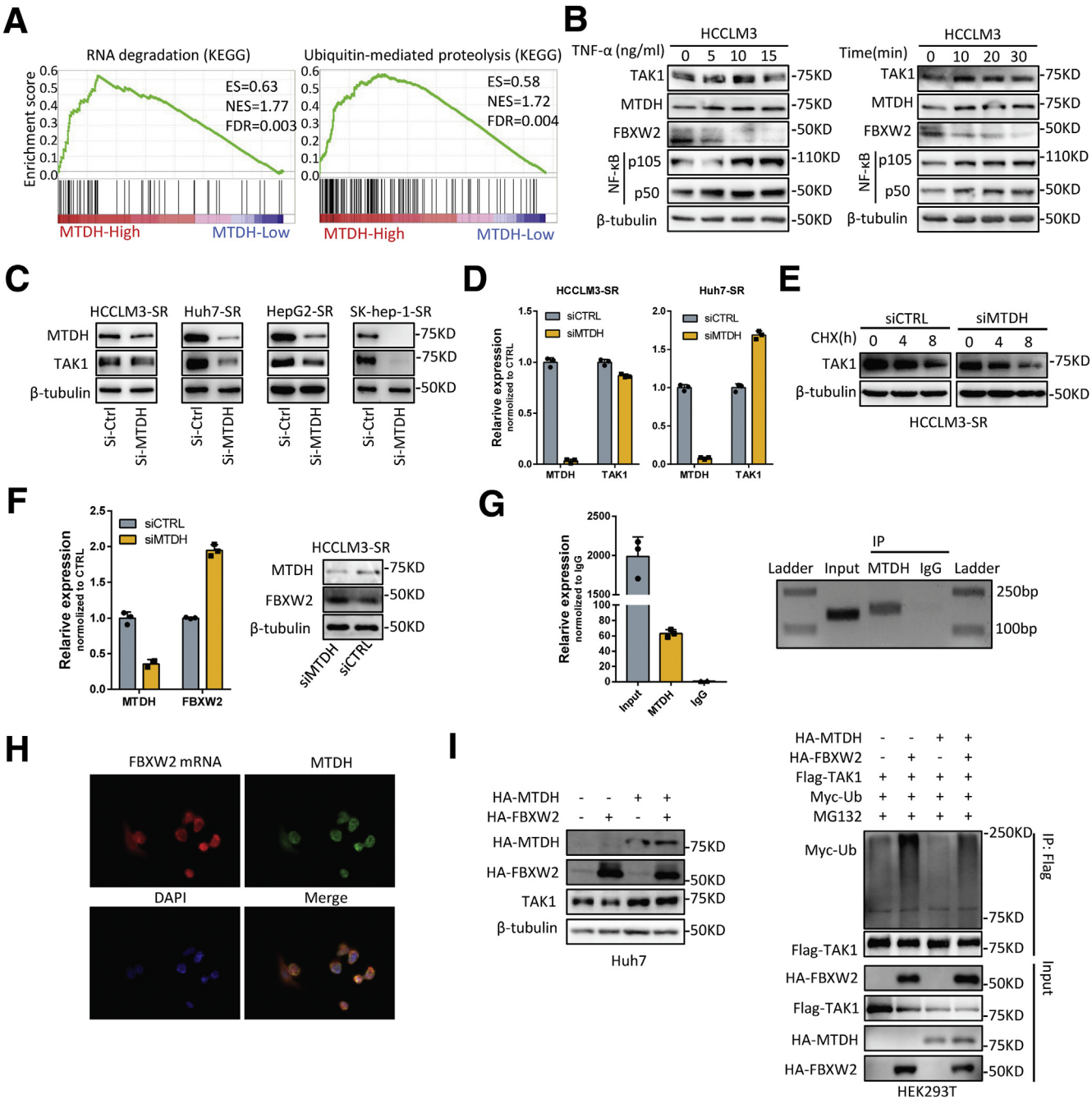

Figure 9. MTDH functions as an upstream regulator of TAK1. (*A*) KEGG pathways significantly enriched in HCC patients with high expression of MTDH using TCGA data. (*B*) Western blotting analysis of TAK1, MTDH, and FBXW2 expression in HCCLM3 cells in response to TNF-α treatment. (*C* and *D*) RT-qPCR quantification and Western blotting analysis of TAK1 and MTDH expression in SR cells transfected with MTDH siRNA or scramble control. (*E*) Half-life of TAK1 protein in HCCLM3 cells transfected with MTDH siRNA or scramble control. (*F*) RT-qPCR quantification and Western blotting analysis of MTDH and FBXW2 protein expression in HCCLM3 cells transfected with MTDH siRNA or scramble control. (*G*) RIP and RT-qPCR analysis of FBXW2 mRNA binding to MTDH protein compared with immunoglobulin G. (*H*) Immunofluorescence analysis of MTDH and FBXW2 mRNA location in HCCLM3 cells. *Green*, MTDH; *red*, FBXW2 mRNA; *blue*, DAPI. (*I*) Immunoblotting analysis of TAK1 protein and Myc-Ub expression in Huh7 cell lysates transfected with indicated constructs. ES, enrichment score; FDR, false discovery rate; NES, normalized enrichment score.

we found that MTDH overexpression partially reduced TAK1 protein level and reduced K48-polyubiquitylation on FBXW2 transfection (Figure 9*I*), suggesting FBXW2-mediated TAK1 degradation could be mitigated by MTDH. In summary, MTDH regulates TAK1 protein level through binding to and subsequently degrading FBXW2 mRNA.

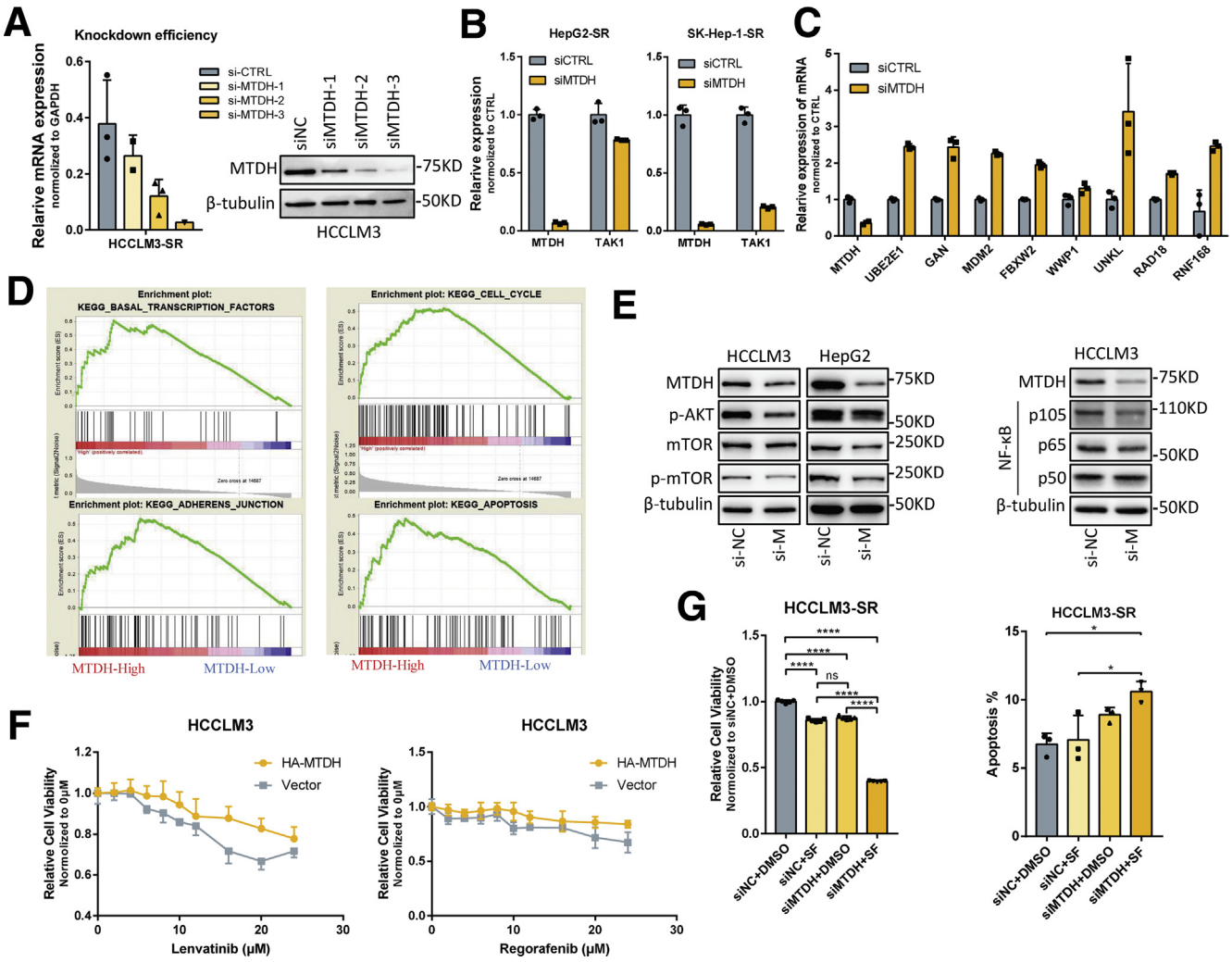

Figure 10. Supplementary data for regulation of TAK1 by MTDH. (*A*) RT-qPCR analysis and Western blotting analysis of MTDH expression in HCCLM3 cells on MTDH knockdown using 3 siRNAs. (*B*) RT-qPCR quantification of TAK1 and MTDH expression in SK-hep-1 and HepG2 cells transfected with MTDH siRNA or scramble control. (*C*) RT-qPCR quantification of E3 mRNAs expression in HCCLM3-SR cells transfected with MTDH siRNA or scramble control. (*D*) KEGG pathways significantly enriched in HCC patients with high expression of MTDH using TCGA data. (*E*) Western blotting analysis of MTDH and NF-κB pathway proteins in HCCLM3-SR and its parental cells; Western blotting analysis of MTDH and AKT pathway proteins in HCCLM3-SR and HepG2-SRs on MTDH knockdown. (*F*) Cell viability of HCCLM3 with stable expression MTDH treated with lenvatinib or regorafenib. (*G*) Relative cell viability and proportion of apoptotic cells in HCCLM3 cells transfected with MTDH siRNA or scramble control in combination with sorafenib or DMSO. Three biological repeats per group.

TAK1 Mediates MTDH-Induced Sorafenib Resistance

To further demonstrate the relationship between MTDH and TAK1, we then aimed to elucidate the function of MTDH in HCC and sorafenib resistance, and whether TAK1 mediates these functions. MTDH has been regarded as a driver oncogene in HCC.[39] Although MTDH has been widely proved to be involved in chemotherapeutics resistance,[17] its role in targeted therapy sensitivity remains unknown. We first used knockdown MTDH by 3 specific siRNAs and found that MTDH knockdown inhibited proliferation of HCC cells, and the third siRNA performed best according to the decrease in cell viability (Figure 11*A*). Knockdown of MTDH also induced apoptosis and cell cycle arrest in G1 phase of HCC cells (Figure 11*B* and *C*). GSEA using TCGA data revealed that MTDH expression was closely related to the regulation of transcription factor activity, cell cycle, apoptosis, mTOR pathways, and TGF-β pathway (Table 1, Figure 10*D*), as indicated by previous studies.[18] Indeed, MTDH suppression reduced classic oncogenic signaling such as p-AKT, p-mTOR, and NF-κB in HCC (Figure 10*E*). We then detected the expression of MTDH in our SR cell models and observed significantly higher protein and mRNA levels of MTDH in SR cells, especially under sorafenib treatment, consistent with the expression alteration of both TAK1 and p-TAK1

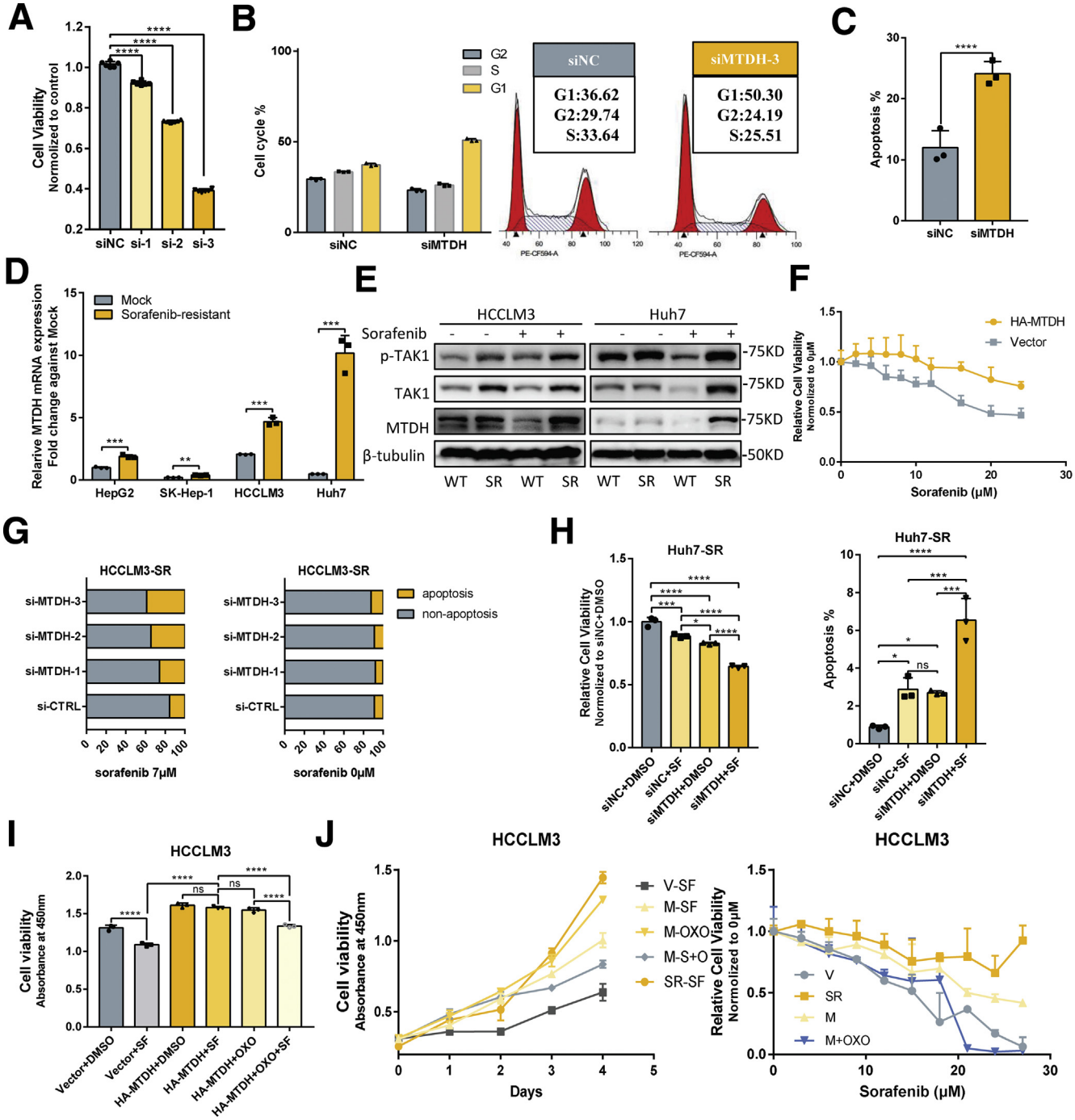

Figure 11. Role of MTDH in HCC and sorafenib resistance. (*A*) Relative cell viability measured by CCK8, (*B*) cell cycle analysis and representative results, and (*C*) proportion of annexin V-stained apoptotic cells analyzed by flow cytometry of HCCLM3 cells transfected with MTDH siRNA or scramble control. Three biological repeats per group. (*D* and *E*) RT-qPCR analysis of MTDH mRNA level and Western blotting analysis of MTDH, TAK1, and p-TAK1 protein level in 4 SR cells compared with their parental cells on sorafenib treatment or not. (*F*) Relative cell viability of HCCLM3 with stable expression MTDH or not treated with increasing dosage of sorafenib. (*G* and *H*) Relative cell viability and proportion of apoptotic cells in HCCLM3 or Huh7 cells transfected with MTDH siRNA or scramble control in combination with sorafenib or DMSO. Three biological repeats per group. (*I*) Relative cell viability of HCCLM3 with stable expression MTDH or not treated with sorafenib and OXO alone or in combination for 48 hours. (*J*) Relative cell viability of HCCLM3 with stable expression MTDH or not treated with OXO or NG25 alone or in combination sorafenib of increasing dosage or for indicated time periods. Three biological repeats per group.

Table 1. KEGG gene sets enriched in MTDH -high HCC patients in TCGA dataset

Name	Size	ES	NES	NOM *P* value	FDR q value
KEGG_AMINOACYL_TRNA_BIOSYNTHESIS	41	0.646	1.774	<.001	0.005
KEGG_RNA_DEGRADATION	57	0.626	1.769	<.001	0.003
KEGG_UBIQUITIN_MEDIATED_PROTEOLYSIS	133	0.579	1.724	<.001	0.004
KEGG_SPLICEOSOME	124	0.572	1.687	<.001	0.005
KEGG_BASAL_TRANSCRIPTION_FACTORS	35	0.606	1.637	.001	0.010
KEGG_NOD_LIKE_RECEPTOR_SIGNALING_PATHWAY	61	0.551	1.571	<.001	0.028
KEGG_CELL_CYCLE	124	0.518	1.536	<.001	0.043
KEGG_ADHERENS_JUNCTION	73	0.534	1.531	<.001	0.041
KEGG_EPITHELIAL_CELL_SIGNALING_IN_HELICOBACTER_PYLORI_INFECTION	67	0.530	1.520	<.001	0.042
KEGG_HOMOLOGOUS_RECOMBINATION	28	0.569	1.516	.009	0.040
KEGG_CHRONIC_MYELOID_LEUKEMIA	73	0.511	1.476	<.001	0.064
KEGG_INOSITOL_PHOSPHATE_METABOLISM	54	0.519	1.467	.005	0.067
KEGG_MTOR_SIGNALING_PATHWAY	52	0.518	1.460	.002	0.067
KEGG_PATHOGENIC_ESCHERICHIA_COLI_INFECTION	55	0.506	1.440	.004	0.082
KEGG_APOPTOSIS	86	0.485	1.415	.001	0.093
KEGG_NEUROTROPHIN_SIGNALING_PATHWAY	126	0.476	1.412	<.001	0.091
KEGG_ENDOCYTOSIS	178	0.469	1.412	<.001	0.087
KEGG_PANCREATIC_CANCER	70	0.493	1.409	.002	0.087
KEGG_SMALL_CELL_LUNG_CANCER	84	0.484	1.407	.002	0.084
KEGG_ACUTE_MYELOID_LEUKEMIA	57	0.491	1.403	.009	0.077
KEGG_RENAL_CELL_CARCINOMA	70	0.482	1.394	.005	0.081
KEGG_OOCYTE_MEIOSIS	111	0.468	1.393	.002	0.079
KEGG_TGF_BETA_SIGNALING_PATHWAY	85	0.476	1.380	.004	0.089

ES, enrichment score; FDR, false discovery rate; NES, normalized enrichment score; NOM, nominal.

(Figure 11*D* and *E*). To verify the role of MTDH in targeted-therapy resistance, we carried out functional experiments to assess the relationship between MTDH and the IC50 of several targeted drugs including sorafenib, regorafenib, and lenvatinib. The results showed that IC50 of these 3 drugs, especially sorafenib, was higher in HCC cells that stably expressed MTDH (Figure 10*F*, Figure 11*F*). We then combined MTDH knockdown and sorafenib treatment in SR cells to further evaluate the function of MTDH in sorafenib resistance. Results showed that MTDH knockdown enhanced sensitivity of SR cells to sorafenib-induced apoptosis and inhibitory of proliferation (Figure 10*G*, Figure 11*G* and *H*). Sorafenib or MTDH knockdown alone also induced apoptosis in SR cells, although the proportion of apoptotic cells remains low. This may be due to the heterogeneity of SR cells and the essential function of MTDH in HCC cell proliferation.

Next we aimed to explore whether TAK1 is involved in MTDH-mediated sorafenib resistance. Consistent with previous findings, HCC cells with ectopically expressed MTDH became more resistant to sorafenib, and such resistance could be reversed by sorafenib in combination with OXO or NG-25, another TAK1 inhibitor (Figure 11*I* and *J*). These data suggested the functional relationship between MTDH and TAK1 in sorafenib resistance.

MTDH and TAK1 Are Both Correlated With Poor Survival of HCC Receiving Sorafenib

To unravel the clinical significance of TAK1 and MTDH, we used immunohistochemistry (IHC) to stain the TAK1 and MTDH protein in tumor samples from 59 HCC patients who underwent surgery before sorafenib treatment. Representative images indicated that HCC patients with high MTDH expression might also have higher TAK1 protein level (Figure 12*A*). Further IHC scoring and statistical analysis revealed that high MTDH expression significantly correlates with high TAK1 protein level (Figure 12*B*). Those patients were then stratified into 2 groups on the basis of TAK1 or MTDH protein level via IHC scoring. Further Kaplan–Meier survival analysis revealed that HCC patients with higher level of TAK1 or MTDH expression had shorter overall survival and DFS (Figure 12*C*). Taken together, these data indicated that TAK1 and MTDH were involved in the development of sorafenib resistance, and their expression positively correlates with each other and predicts sorafenib response in HCC patients.

Discussion

Most HCC patients are diagnosed at an advanced stage when surgical approaches and locoregional therapies are no

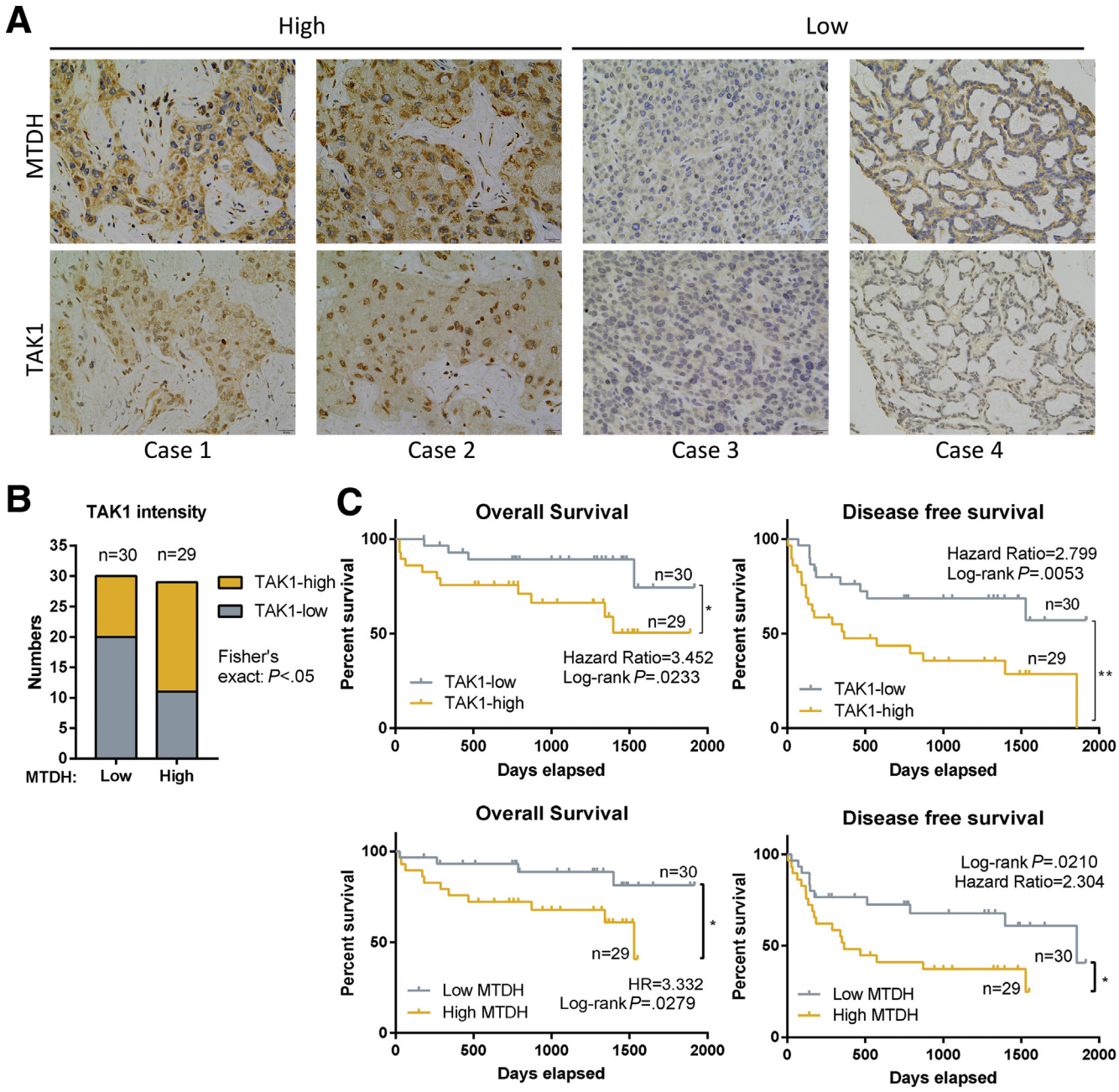

Figure 12. MTDH/TAK1 expression in HCC patients receiving sorafenib. (*A*) Representative images of MTDH and TAK1 immunohistochemical staining in HCC patients receiving sorafenib before surgery. (*B*) Correlation between MTDH and TAK1 staining. Significance was determined using χ^2 (and Fisher exact) test. (*C*) Kaplan-Meier survival curves of these patients with low or high TAK1 or MTDH staining. Significance was determined using Kaplan-Meier analyses. Survival analysis was performed using log-rank test.

longer feasible. Improvements in patient outcomes from most systematic therapies have been modest, although several targeted drugs and immune checkpoint inhibitors have been proved effective in the last decade,[40] and more combinational strategies are being explored.[41] The underlying mechanisms of sorafenib resistance remain complex and largely unknown. To better address this critical problem, we had established acquired SR HCC cell models by treating HCC cells with increasing concentrations of sorafenib in culture media over time.[6,21] On the basis of these models, our previous studies had proved the crucial role of androgen receptor signals, EMT-related transcriptional factors, and several non-coding RNAs in sorafenib resistance, highlighting the epigenetic regulation of driver oncogenes in sorafenib resistance.[5,6,42–45] However, therapy-induced tumor cell evolving is comprehensive and systematic in terms of cellular and molecular alteration. Thus, identifying other novel targets still remains an unmet medical need, requiring new insights into underlying molecular mechanisms that support hepatocarcinogenesis, HCC progression, and drug

resistance based on genomic, transcriptomic, and epigenomic studies.

In our study, some issues had been raised about SR cell models. We previously reviewed that EMT and cancer stem cells are common mechanisms underlying acquired sorafenib resistance. However, SR cells in our study underwent atypical EMT process that not all EMT markers and EMT-related transcriptional factors altered accordingly especially E-cadherin, although SR cells exhibited mesenchymal-like morphologic changes. Recent studies revealed that EMT is a processive program, and there are tumor cells undergoing intermediate EMT process. Actually, such EMT heterogeneity has already been proposed and remains controversial in recent years.[46] Cells express CDH1 (encodes E-cadherin) but do not display E-cadherin at the cell surface, cells with partially mesenchymal features but without evident expression of EMT-related transcriptional factors, and so on had been reported.[47,48] Another possible reason is that E-cadherin might be asymmetrically distributed toward the cell surfaces.[49] Padmanaban et al[28] found that E-cadherin promotes metastasis through limiting reactive oxygen-mediated apoptosis in breast ductal carcinomas. To this point, E-cadherin itself might have uncovered roles in our SR model. We found that SR cells tend to be clustered under sorafenib treatment, and stemness marker staining also indicated that the stem cells are located in the core of such "cluster". It is possible that E-cadherin mediates cell-to-cell connection during SR cell clustering, but further experiments are required to demonstrate this hypothesis. Not all SR cells exhibited stemness features, which is consistent with EMT heterogeneity mentioned above. Such heterogeneity may also lead to functional heterogeneity of SR cells, that is, during cell proliferation and division, some SR cell subpopulation may lose sorafenib resistance. This may explain why sorafenib alone could still induce apoptosis in SR cells, although it remains a very low ratio.

Recently in many other tumor entities, TAK1 has been considered a robust therapeutic target especially in lung, colon, and pancreatic cancers, most of which exhibit frequent KRAS mutations.[50,51] Although artificial TAK1-deletion leads to early onset of hepatocarcinogenesis in liver, HCC patients rarely harbor TAK1-deletion mutations according to TCGA database. Moreover, we observed that HCC specimens harbor higher TAK1 mRNA expression, which was increasing from early-stage to advanced-stage HCC patients. Metabolic syndrome together with alcohol abuse and hepatitis C infection contribute to the increasing incidence and death rate of liver cancers including HCC.[52] From an etiologic perspective, recent studies indicated that TAK1 promoted NASH and NAFLD.[15,16,53] The role of TAK1 in inflammation-driven HCC including hepatic steatosis and virus infection might be attributed to TNF-α stimulation, which was also indicated to be potential target to overcome sorafenib resistance recently.[35] These clues prompted us to explore the role of TAK1 in developed HCC, especially in HCC progression and therapy resistance. Indeed, we found elevated protein levels of TAK1 in HCC patients, HCC cell lines, and SR cell models, and its expression predicts poor patient outcomes. In vivo and in vitro assay also suggested that genetic knockdown and pharmacologic inhibition of TAK1 using inhibitors OXO or NG-25 significantly suppressed cell proliferation and tumor growth and overcame sorafenib resistance. But it is never too cautious to make the conclusion that TAK1 is a therapeutic target for HCC.

Because TAK1 deletion could cause spontaneous hepatocarcinogenesis, it is worthy of discussion about whether pharmacologic TAK1 inhibition could induce detrimental effect. First, we believed that TAK1 deletion and pharmacologic TAK1 inhibition are totally different conditions. The latter one only inhibits the phosphorylation of TAK1 in HCC cells and will not completely eliminate all TAK1 protein, which could continue to play essential functions. In addition, TAK1 inhibitors have been applied in other tumor models by many studies, but none reported spontaneous hepatocarcinogenesis in mice liver. Of course, it is also possible that the authors were not aware of this issue, or the duration of TAK1 inhibitors treatment is too short to induce hepatocarcinogenesis. Because of role of TAK1 in steatohepatitis, TAK1 inhibitor was also used to treat HFD (High fat diet)-induced NAFLD in DUSP14-ko mice, and hepatocarcinogenesis was not reported in this model.[54] Moreover, TAK1 deletion induced hepatocarcinogenesis was not attributed to the inhibition of antiproliferative role of TAK1 but cell death-induced inflammation and compensatory mechanisms, for instance, promoting macrophage infiltration.[55] Last, genetic TAK1 deletion in liver is artificial, and TAK1-deficiency induced hepatocarcinogenesis in natural conditions had not been reported. All in all, the function of TAK1 is context-dependent. In our study, we focused on the status of TAK1 in transformed malignant HCC cells and its role in subsequent tumor progression and treatment resistance, which may not be in conflict with the role of TAK1 deletion in nonmalignant hepatocytes.

This study also explored the regulatory mechanism of TAK1 expression. We observed that sorafenib treatment reduced total protein of TAK1 in HCC cells, suggesting TAK1 is a direct or indirect target of sorafenib. Sorafenib as well as other tyrosine kinase inhibitors are well-known to inhibit Ras/MEK/ERK and PI3K/Akt/mTOR pathways. Previous research demonstrated that TAK1 functions in a KRAS-dependent way in other tumor entities especially in pancreatic adenocarcinoma. Sorafenib inhibits non-small-cell lung cancer cell growth by targeting B-RAF in cells with wild-type KRAS and C-RAF in those with mutant KRAS.[56] We knocked down KRAS expression using siRNA and inhibited AKT function using selective inhibitor in HCC cells. The Western blotting results showed that KRAS knockdown and AKT inhibitor both decreased the total TAK1 expression (data not shown). Hence, sorafenib might down-regulate TAK1 expression through Ras/MEK/ERK and PI3K/Akt/mTOR pathways. One study also proved that sorafenib inhibited ATP-binding of TAK1 using in situ kinome.[57] Although the function of TAK1 and FBXW2 binding to TAK1 depends on specific site phosphorylation or dephosphorylation, it is possible that sorafenib regulates TAK1 level through inhibiting corresponding phosphorylation kinases. Altogether, the mechanistic reason for the

Table 2. Lists of Primers for Constructs

Target gene	Forward primer	Reverse primer
HA-BTRC	GTTCCAGATTACGCTGAATTCATGGACCCGGCCGAGG	CAGGTCGACTCTAGAGGATCCTTATCTGGAGATGTAGGTGTATGTTCGAGAAG
HA-FBXW2	GTTCCAGATTACGCTGAATTCATGGAGAAAGGACTTTGAGACATGG	CAGGTCGACTCTAGAGGATCCTCAGCCGTGCTCCTTCCAC
HA-FBXW4	GTTCCAGATTACGCTGAATTCATGGCGGCGGCGGCCGGGGAGGAGG	CAGGTCGACTCTAGAGGATCCTCATGGGTTTTGAAAATCCAGGACG
HA-FBXW5	GTTCCAGATTACGCTGAATTCATGGGCCTGTCGCCC	CAGGTCGACTCTAGAGGATCCTCAGCGCCTCTGGCTGG
HA-FBXW7	GTTCCAGATTACGCTGAATTCATGTGTGTCCCGAGAAGCG	CAGGTCGACTCTAGAGGATCCTCACTTCATGTCCACATCAAAGTCCAG
HA-FBXW8	GTTCCAGATTACGCTGAATTCATGGACGACTACAGCCTGGATG	CAGGTCGACTCTAGAGGATCCCTAAACATGGTTATAGGGAAAGGCCAGT
HA-FBXW11	GTTCCAGATTACGCTGAATTCATGGAGCCCGACTCGGT	CAGGTCGACTCTAGAGGATCCTTATCTAGAGATGTAAGTGTATGTTCTGGAGGG
HA-FBXW12	GTTCCAGATTACGCTGAATTCATGAGCCCCCACTCACCAGAT	CAGGTCGACTCTAGAGGATCCTTACGTATTCAAAGAATACATCACCAGAATGCT
HA-FBXO4	GTTCCAGATTACGCTGAATTCATGGCGGGAAGCGAGC	CAGGTCGACTCTAGAGGATCCTCATCTTGCACGCTTAGATTCCACT
HA-FBXL3	GTTCCAGATTACGCTGAATTCATGAAACGAGGAGGAAGAGATAGTGACC	CAGGTCGACTCTAGAGGATCCTTACCAAGTGGGCATCATGTCG
HA-MTDH	GTTCCAGATTACGCTGAATTCATGGCTGCACGGAGCT	CAGGTCGACTCTAGAGGATCCTCACGTTTCTCGTCTGGC
Myc-FBXW2	CTCGGTTCTATCGATGCCACCATGGAGCAGAAACTCATCTCTGAAGA GGATCTGATGGAGAGAAAGGACTTTGAGA	TCTGATATCGAATTCTCAGCCGTGCTCCTTCCA
Flag-TAK1	GATGATGACGACAAGGAATTCATGTCTACAGCCTCTGCCGC	CAGGTCGACTCTAGAGGATCCTCATGAAGTGCCTTGTCGTTTC

decreased levels of TAK1 on sorafenib treatment might be more diverse and is in need for further study.

However, it is the TAK1 protein level but not mRNA expression that was elevated in SR cells and was retained even under sorafenib treatment. Although most studies focus on K63-polyubiquitylation-dependent activation of TAK1,[11,58] these data lead us to explore which E3 ligase mediates K48-linked degradation of TAK1. F-box proteins mediate the degradation of a large number of regulatory proteins involved in diverse processes and have emerging roles in cancer and drug resistance.[31,59] Previous study identified FBXW5 as a functional suppressor rather than an expression regulator for TAK1.[60] We used IP assays and identified FBXW2 as a novel E3 ligase targeting TAK1 for K48-linked ubiquitylation and subsequent degradation through specific degron sequences. Our results also revealed that FBXW2 is not the only F-box protein that could bind to TAK1, regardless of nonspecific binding to tag beads. It is not surprising that other F-box proteins also regulate TAK1 activation and protein degradation because TAK1 is a gatekeeper of cellular homeostasis and must be under tight regulation. However, how other F-box proteins regulate TAK1 needs further investigation. Moreover, some issues remain unexplored in this study including how FBXW2 recruits the substrate TAK1, whether such recruitments depend on degron phosphorylation, and which kinases are responsible for the degron phosphorylation.

MTDH has been identified as a master and actionable gene in HCC as well as other tumor entities. It functions as a downstream mediator of the transforming activity of oncogenic Ha-Ras and c-Myc and activates MAPK, PI3K/Akt, NF-κB, and Wnt/β-catenin signaling pathways.[18] Several studies have demonstrated that MTDH is an RNA-binding protein and could bind to many E3 or E2 mRNAs including FBXW2 and regulate their stability or translation.[36,38] Furthermore, MTDH and TAK1 function similarly in tumor progression and therapy resistance, respond to overlapped stimuli, and activate common downstream pathways.[7,17] Our expression analysis and functional experiments also proved that MTDH is essential for HCC development and sorafenib resistance. These findings and clues suggested that MTDH might be a potential upstream regulator for TAK1 at post-translational level. Indeed, our findings suggested that MTDH regulates TAK1 protein level through binding to FBXW2 mRNA and promoting its degradation. However, pharmacologic suppression of MTDH that is based on neither druggable structure nor bioactive compounds remains achievable. This study also proved that targeting TAK1 reversed MTDH-dependent and -independent sorafenib resistance in vitro and in vivo. In summary, MTDH overexpression in SR cells retarded the degradation of TAK1 protein and thus mitigated the inhibitory effect from sorafenib on TAK1. However, how long-term sorafenib treatment resulted in up-regulation of MTDH is still unknown and has not been elucidated in this study. Taken together, present study identified the MTDH/FBXW2/TAK1 axis, which is important in HCC progression and sorafenib resistance, and provided evidence for TAK1 as a robust therapeutic target in HCC and MTDH-dependent or

Table 3. List of siRNAs

Target	Sense	Anti-sense
siTAK1	GCAGUGAUUCUUGGAUUGU	ACAAUCCAAGAAUCACUGC
siFBXW2-1	GCAGCGGUGAAGUUUGAUGAA	UUCAUCAAACUUCACCGCUGC
siFBXW2-2	GCCUUUGAAACCUCGUCAU	AUGACGAGGUUUCAAAGGC
siMTDH-1	GGAGGAGGCUGGAAUGAAA	UUUCAUUCCAGCCUCCUCC
siMTDH-2	CAGAUAAAUCCAAGUCAAA	UUUGACUUGGAUUUAUCUG
siMTDH-3	CUUAGUGAAUUGUGAUAAAGAAA	UUUCUUUAUCACAAUUCACUAAGUGAU

-independent sorafenib resistance, rendering further preclinical and clinical studies to explore.

Materials and Methods

Cell Culture and Transfections

Human embryonic kidney 293 (HEK293) cells, Huh7, HepG2, SK-hep-1, HCCLM3, HLF, SMMC7721, JHH7, PLC/PRF/5, and Ha22T cells, normal liver L02 and Chang cells were obtained from the American Type Culture Collection and were maintained in Dulbecco modified Eagle medium containing 10% (v/v) fetal bovine serum at 37°C in 5% CO_2 condition. All cell lines were routinely tested to be negative for mycoplasma contamination. Transfection of siRNA and plasmids was performed using Lipofectamine 3000 Reagents (Thermo Fisher Scientific, Waltham, MA) following the manufacturer's instructions.

Bioinformatic Analysis and GSEA

HCC datasets were downloaded from TCGA data portal (http://www.tcga-data.nci.nih.gov). MAP3K7 (TAK1) and MTDH mRNA levels were analyzed from TCGA and NCBI GEO databases (https://www.ncbi.nlm.nih.gov). For TCGA data, 5 of 374 HCC patients were excluded because of the absence of follow-up data. Finally, 369 HCC patients were subjected to mRNA expression in our analysis. GSEA was used to analyze whether a series of defined KEGG gene sets show statistically significant, concordant differences between 2 groups stratified on the basis of MTDH expression of HCC cases in TCGA dataset.

Plasmids, SiRNAs, and Reagents

HA-MTDH, HA-β-TrCP1, HA-FBXW2, HA-FBXW4, HA-FBXW5, HA-FBXW7, HA-FBXW8, HA-FBXW11, HA-FBXW12, HA-FBXL3, and HA-FBXO4 expression plasmids were subcloned with N-terminal double HA tags into pXF4H expression vector between the BamHI and EcoRI restriction sites. Flag-TAK1 was constructed with N-terminal triple Flag tags into pXF6F expression vector between the BamHI and EcoRI restriction sites. Myc-FBXW2 was constructed with N-terminal Myc tag into Pxf4H expression vector between the ClaI and EcoRI sites. All vectors and Myc-Ub were gifts from Lidan Hou. PCR and plasmids construction were performed using 2× Phanta Max Master Mix (#P511) and ClonExpress II One Step Cloning Kit (#C112) purchased from Vazyme Biotech Co, Ltd, Nanjing, China according to the manufacturer's instructions. The primers used to generate the above cDNA fragments were purchased from Tsingke, Beijing, China and are shown in Table 2. The pooled siRNA oligos targeting for MTDH, TAK1, and FBXW2 were purchased from Guangzhou RiboBio Co, Ltd (Guangzhou, China), and the sequences of siRNA oligos are shown in Table 3. Sorafenib and MG132 were purchased from MedChemExpress (Princeton, NJ). OXO was purchased from MedChemExpress. APExBio, Cayman, and CHX were purchased from Beyotime Biotechnology (Nanjing, China). Puromycin (Solarbio, Beijing, China; P8230) was purchased from Solarbio. MLN4924 was a gift from Lidan Hou (Zhejiang University). Apoptosis (70-AP101) and Cell Cycle Assay (70-CCS012) were purchased from Multi Science, Beijing, China. Cell Counting Kits (40203ES60) were purchased from Yeasen Biotechnology, Shanghai, China. DAPI solution (C0060) and Mounting Medium (S2110) were purchased from Solarbio.

IP and Immunoblotting

Cells were lysed in an IP lysis buffer (150 mmol/L NaCl, 1% NP-40, 50 mmol/L Tris-HCl, pH 8.0, 1 mmol/L

Table 4. List of Antibodies for Indicated Uses

Target gene	Catalog no.	Producer	Target gene	Catalog no.	Producer
Anti-TAK1	Ab109526	Abcam	Anti-TAK1	#5206S	CST
Anti-TAK1 (p-S439)	Ab109404	Abcam	Anti-LYRIC	Ab227981	Abcam
Anti-FBXW2	11499-1-AP	ProteinTech	Anti-CUL1	Ab75817	Abcam
Anti-Flag	F3165	Sigma-Aldrich	Anti-SKP1	Ab76502	Abcam
Anti-HA	H6908	Sigma-Aldrich	EMT Kit	9782	CST
Anti-Myc	Ab32	Abcam			

Table 5. List of Primers for qPCR

Target	Forward primer	Reverse primer
MTDH	AAGGAGATTCTACACTTCAGGTTTC	TTCCAGCCTCCTCCATTGAC
TAK1	ATTGTAGAGCTTCGGCAGTT	TATATAAAGAGCCCCCTTCAGC
FBXW2	CGGGGGCGGTGTTCAGT	AGCCCATACTTTCACAGCGA
GAPDH	GTCTTCACCACCATGGAGAAGG	ATGATCTTGAGGCTGTTGTCAT
Bcl-2	CAGGATAACGGAGGCTGGGATG	AGAAATCAAACAGAGGCCGCA
GADD45B	CTGGTCACGAACCCTCACAC	CTTTCTTCGCAGTAGCTGGC
UBE2E1	AGTTGCTGTTGCTGCACTTC	AACAGCCCCTCTCTTTGTGTC
GAN	AGCCCGTACATCAGGACAAAG	TGATCTGCCCACTGAAGATGT
RNF168	AACGTGGAACTGTGGACGAT	GTCATCAGCCACTTCCTCTGA
RAD18	TTTTGCACGGAATCATCTGCTG	TTAACCTGCTCCCCTGCTTT
MDM2	CAGTAGCAGTGAATCTACAGGGA	CTGATCCAACCAATCACCTGAAT
UNKL	TGGCAAGATGCCAACTTCGT	GTGGACCTGTACTGGAACCG
WWP1	ACTGCAGCTCATCTCCAACC	TTCAACAGCCAACCTGGCA

Na3VO4), supplemented with complete protease inhibitor cocktail (EDTA free, mini-Tablet; MedChemExpress). For IP, 1–2 mg lysates were incubated with bead-conjugated FLAG, MYC, or HA (Sigma-Aldrich) or the appropriate antibody (2 μg) in a rotating incubator overnight at 4°C, followed by 2-hour incubation with Protein-A Sepharose beads (Santa Cruz Technology, Santa Cruz, CA). Immunocomplexes were washed 4 times with TBST or IP lysis buffer before resolved by sodium dodecyl sulfulate-polyacrylamide gel electrophoresis and analyzed by immunoblotting. For direct IB analysis, cells were lysed in lysis buffer (50 mmol/L Tris-HCl, pH 8.0, 150 mmol/L NaCl, 1% TritonX-100, 1% sodium deoxycholate, and 0.1% sodium dodecyl sulfate, 1 mmol/L EDTA). Proteins were resolved on sodium dodecyl sulfate polyacrylamide gels and then transferred to a polyvinylidene difluoride membrane. After blocking with 5% (w/v) milk or bovine serum albumin, the membrane was stained with the corresponding primary antibodies that are shown in Table 4. All antibodies were diluted in Primary Antibody Dilution Buffer (Solarbio, A1810).

RNA Extraction and Real-Time PCR

Cells were transiently transfected with indicated plasmids or siRNA for 24–48 hours, and the total RNA was then isolated using TRIzol Reagent (15596-018; Invitrogen, Carlsbad, CA). The concentration of RNA was measured by NanoDrop 2000. Total RNA was then transcribed into complementary DNA using Hifair II 1st Strand cDNA Synthesis Kit (11121ES60, Yeasen Biotechnology) according to the manufacturer's protocol. The quantification of complementary DNA was performed using SYBR Green Master Mix (11201ES08-5, Yeasen Biotechnology) on LightCycler 480 (Roche, Basel, Switzerland). The housekeeping gene, glyceraldehyde-3-phosphate dehydrogenase, was used as a loading control. The sequences of primer sets are shown in Table 5.

Half-Life Analysis

After gene manipulation, 100 μg/ml CHX (Beyotime) was added to the cell medium. At the indicated time points, cells were harvested, lysed, and subjected to Western blotting analysis. The densitometry quantification was performed using Image Lab Processing software (Bio-Rad, Hercules, CA).

In Vivo Antitumor Study

Four- to five-week-old BALB/c athymic nude mice (nu/nu, male) were purchased from Shanghai SLAC Laboratory Animal Centre. Mice were fed with a regular diet and had free access to water and food. All mice procedures were approved by the Sir Run-Run Shaw Hospital Committee on Use and Care of Animals. The cell line–derived xenograft and orthotopic models were constructed as described below. Around 5×10^6 HCCLM3-SR cells were mixed with phosphate-buffered saline in a total volume of 0.2 mL and were then subcutaneously injected into both flanks of mice. When the tumors reached a volume of ~500 mm^3, the mice were then killed, and the tumors were cut into small pieces evenly and replanted into 1 flank of mice. Those mice were then divided into 2 groups. To maintain the sorafenib resistance in HCCLM3-SR–derived tumors, sorafenib (25 mg/kg, oral) was given once a day in one group, whereas the other group received only vehicle as control. Two weeks later, the xenograft tumor volume was compared between 2 groups, and SR tumors were then chosen and replanted into the flank of mice or liver of mice to construct xenograft or orthotopic models. The abdomen of the nude mice was touched to determine the size of the tumor every week. When the tumors reached ~100 mm^3, mice were then randomized into 4 groups (6 mice per group). Sorafenib (25 mg/kg, oral) was given once a day; OXO (20 mg/kg, intraperitoneal) was administered every 2 days; mice of the control group received only dimethyl sulfoxide (DMSO) as the vehicle control. The growth of tumors was measured at

the indicated time points, and average tumor volumes were calculated according to the equation, Volume = (Length × Width × Width)/2. After 2 weeks, mice were killed, and all the tumor tissues were collected, fixed, and sectioned.

Human Specimens and Immunohistochemical Staining

Human HCC tumor tissue microarrays data were purchased from Shanghai Xinchao Biotech, China. For immunohistochemical staining, the sections were deparaffinized in xylene and rehydrated through graded ethanol. Antigen retrieval was performed for 20 minutes at 100°C with 0.1% sodium citrate buffer (pH 6.0). After quenching of endogenous peroxidase activity with 3% $H_2O_2 \cdot dH_2O$ and blocking of nonspecific binding with 5% goat serum albumin buffer, sections were incubated overnight at 4°C with indicated antibodies. After 3 times washes of phosphate-buffered saline, the sections were treated with horseradish peroxidase conjugated secondary antibody for 30 minutes at room temperature and stained with 0.05% 3, 3-diaminobenzidine tetrahydrochloride. Slides were photographed with virtual slide microscope. Quantification of the immunohistochemical staining was conducted on the basis of the ratio and intensity of the staining.

Statistical Analysis

Results are expressed as mean ± standard error of the mean. The Student t test was used for comparison between 2 groups. One-way analysis of variance was used for comparisons between the means of 3 or more groups. The Tukey test, Bonferroni test, or Dunnett test were used for post multiple comparisons between groups. For analysis of tissue microarrays, the Fisher exact test was used. The level of significance was $P < .05$ ($^*P < .05$, $^{**}P < .01$, and $^{***}P < .001$). The number of independent experiments was n ≥3 (if not depicted otherwise). Calculations were performed using the GraphPad Prism Software (San Diego, CA).

References

1. Bray F, Ferlay J, Soerjomataram I, Siegel RL, Torre LA, Jemal A. Global cancer statistics 2018: GLOBOCAN estimates of incidence and mortality worldwide for 36 cancers in 185 countries. CA Cancer J Clin 2018; 68:394–424.
2. Gao Q, Zhu H, Dong L, Shi W, Chen R, Song Z, Huang C, Li J, Dong X, Zhou Y, Liu Q, Ma L, Wang X, Zhou J, Liu Y, Boja E, Robles AI, Ma W, Wang P, Li Y, Ding L, Wen B, Zhang B, Rodriguez H, Gao D, Zhou H, Fan J. Integrated proteogenomic characterization of HBV-related hepatocellular carcinoma. Cell 2019;179:1240.
3. Xu LX, He MH, Dai ZH, Yu J, Wang JG, Li XC, Jiang BB, Ke ZF, Su TH, Peng ZW, Guo Y, Chen ZB, Chen SL, Peng S, Kuang M. Genomic and transcriptional heterogeneity of multifocal hepatocellular carcinoma. Ann Oncol 2019.
4. Xia S, Pan Y, Liang Y, Xu J, Cai X. The microenvironmental and metabolic aspects of sorafenib resistance in hepatocellular carcinoma. EBioMedicine 2020:51.
5. Xu J, Zheng L, Chen J, Sun Y, Lin H, Jin RA, Tang M, Liang X, Cai X. Increasing AR by HIF-2alpha inhibitor (PT-2385) overcomes the side-effects of sorafenib by suppressing hepatocellular carcinoma invasion via alteration of pSTAT3, pAKT and pERK signals. Cell Death Disease 2017;8:e3095.
6. Lin Z, Xia S, Liang Y, Ji L, Pan Y, Jiang S, Wan Z, Tao L, Chen J, Lin C, Liang X, Xu J, Cai X. LXR activation potentiates sorafenib sensitivity in HCC by activating microRNA-378a transcription. Theranostics 2020; 10:8834–8850.
7. Santoro R, Carbone C, Piro G, Chiao PJ, Melisi D. TAKing aim at chemoresistance: the emerging role of MAP3K7 as a target for cancer therapy. Drug Resistance Updates 2017;33–35:36–42.
8. Mukhopadhyay H, Lee NY. Multifaceted roles of TAK1 signaling in cancer. Oncogene 2020;39:1402–1413.
9. Inokuchi S, Aoyama T, Miura K, Österreicher CH, Kodama Y, Miyai K, Akira S, Brenner DA, Seki E. Disruption of TAK1 in hepatocytes causes hepatic injury, inflammation, fibrosis, and carcinogenesis. Proc Natl Acad Sci 2010;107:844–849.
10. Yang L, Inokuchi S, Roh YS, Song J, Loomba R, Park EJ, Seki E. Transforming growth factor-b2: signaling in hepatocytes promotes hepatic fibrosis and carcinogenesis in mice with hepatocyte-specific deletion of TAK1. Gastroenterology 2013;144:1042–1054.e4.
11. Yan F-J, Zhang X-J, Wang W-X, Ji Y-X, Wang P-X, Yang Y, Gong J, Shen L-J, Zhu X-Y, Huang Z, Li H. The E3 ligase tripartite motif 8 targets TAK1 to promote insulin resistance and steatohepatitis. Hepatology 2017; 65:1492–1511.
12. Mitra A, Yan J, Xia X, Zhou S, Chen J, Mishra L, Li S. IL6-mediated inflammatory loop reprograms normal to epithelial-mesenchymal transition+ metastatic cancer stem cells in preneoplastic liver of transforming growth factor beta–deficient β2-spectrin+/− mice. Hepatology 2017;65:1222–1236.
13. Zhao N, Wang R, Zhou L, Zhu Y, Gong J, Zhuang SM. MicroRNA-26b suppresses the NF-κB signaling and enhances the chemosensitivity of hepatocellular carcinoma cells by targeting TAK1 and TAB3. Mol Cancer 2014;13:35.
14. Roh YS, Song J, Seki E. TAK1 regulates hepatic cell survival and carcinogenesis. J Gastroenterol 2014; 49:185–194.
15. Zhao Y, Wang F, Gao L, Xu L, Tong R, Lin N, Su Y, Yan Y, Gao Y, He J, Kong L, Yuan A, Zhuge Y, Pu J. Ubiquitin-specific protease 4 is an endogenous negative regulator of metabolic dysfunctions in nonalcoholic fatty liver disease in mice. Hepatology 2018;68:897–917.
16. Ji Y-X, Huang Z, Yang X, Wang X, Zhao L-P, Wang P-X, Zhang X-J, Alves-Bezerra M, Cai L, Zhang P, Lu Y-X, Bai L, Gao M-M, Zhao H, Tian S, Wang Y, Huang Z-X, Zhu X-Y, Zhang Y, Gong J, She Z-G, Li F, Cohen DE, Li H. The deubiquitinating enzyme cylindromatosis mitigates nonalcoholic steatohepatitis. Nat Med 2018; 24:213–223.

17. Meng X, Thiel KW, Leslie KK. Drug resistance mediated by AEG-1/MTDH/LYRIC. Adv Cancer Res 2013; 120:135–157.
18. Hu G, Wei Y, Kang Y. The multifaceted role of MTDH/AEG-1 in cancer progression. Clin Cancer Res 2009; 15:5615–5620.
19. Ninomiya-Tsuji J, Kajino T, Ono K, Ohtomo T, Matsumoto M, Shiina M, Mihara M, Tsuchiya M, Matsumoto K. A resorcylic acid lactone, 5z-7-oxozeaenol, prevents inflammation by inhibiting the catalytic activity of TAK1 MAPK kinase kinase. J Biol Chem 2003;278:18485–18490.
20. Luedde T, Schwabe RF. NF-κB in the liver: linking injury, fibrosis and hepatocellular carcinoma. Nat Rev Gastroenterol Hepatol 2011;8:108–118.
21. van Malenstein H, Dekervel J, Verslype C, Van Cutsem E, Windmolders P, Nevens F, van Pelt J. Long-term exposure to sorafenib of liver cancer cells induces resistance with epithelial-to-mesenchymal transition, increased invasion and risk of rebound growth. Cancer Lett 2013; 329:74–83.
22. Shibue T, Weinberg RA. EMT, CSCs, and drug resistance: the mechanistic link and clinical implications. Nat Rev Clin Oncol 2017;14:611.
23. Viswanathan VS, Ryan MJ, Dhruv HD, Gill S, Eichhoff OM, Seashore-Ludlow B, Kaffenberger SD, Eaton JK, Shimada K, Aguirre AJ. Dependency of a therapy-resistant state of cancer cells on a lipid peroxidase pathway. Nature 2017;547:453.
24. Zhang J, Zhang Q, Lou Y, Fu Q, Chen Q, Wei T, Yang J, Tang J, Wang J, Chen Y, Zhang X, Zhang J, Bai X, Liang T. Hypoxia-inducible factor-1α/interleukin-1β signaling enhances hepatoma epithelial–mesenchymal transition through macrophages in a hypoxic-inflammatory microenvironment. Hepatology 2018; 67:1872–1889.
25. Zhou S-L, Yin D, Hu Z-Q, Luo C-B, Zhou Z-J, Xin H-Y, Yang X-R, Shi Y-H, Wang Z, Huang X-W, Cao Y, Fan J, Zhou J. A positive feedback loop between cancer stem-like cells and tumor-associated neutrophils controls hepatocellular carcinoma progression. Hepatology 2019; 70:1214–1230.
26. Lin X, Li AM, Li YH, Luo RC, Zou YJ, Liu YY, Liu C, Xie YY, Zuo S, Liu Z, Liu Z, Fang WY. Silencing MYH9 blocks HBx-induced GSK3β ubiquitination and degradation to inhibit tumor stemness in hepatocellular carcinoma. Signal Transduct Target Ther 2020;5:13.
27. Pastushenko I, Brisebarre A, Sifrim A, Fioramonti M, Revenco T, Boumahdi S, Van Keymeulen A, Brown D, Moers V, Lemaire S. Identification of the tumour transition states occurring during EMT. Nature 2018;556:463.
28. Padmanaban V, Krol I, Suhail Y, Szczerba BM, Aceto N, Bader JS, Ewald AJ. E-cadherin is required for metastasis in multiple models of breast cancer. Nature 2019; 573:439–444.
29. Zheng L, Xu M, Xu J, Wu K, Fang Q, Liang Y, Zhou S, Cen D, Ji L, Han W, Cai X. ELF3 promotes epithelial-mesenchymal transition by protecting ZEB1 from miR-141-3p-mediated silencing in hepatocellular carcinoma. Cell Death Disease 2018;9:387.
30. Harding JJ, Nandakumar S, Armenia J, Khalil DN, Albano M, Ly M, Shia J, Hechtman JF, Kundra R, El Dika I, Do RK. Prospective genotyping of hepatocellular carcinoma: clinical implications of next generation sequencing for matching patients to targeted and immune therapies. Clin Cancer Res 2019;25:2116–2126.
31. Wang Z, Liu P, Inuzuka H, Wei W. Roles of F-box proteins in cancer. Nat Rev Cancer 2014;14:233–247.
32. Skaar JR, Pagan JK, Pagano M. Mechanisms and function of substrate recruitment by F-box proteins. Nat Rev Mol Cell Biol 2013;14:369–381.
33. Yang F, Xu J, Li H, Tan M, Xiong X, Sun Y. FBXW2 suppresses migration and invasion of lung cancer cells via promoting β-catenin ubiquitylation and degradation. Nat Commun 2019;10:1382.
34. Yang YM, Kim SY, Seki E. Inflammation and liver cancer: molecular mechanisms and therapeutic targets. Semin Liver Dis 2019;39:26–42.
35. Tan W, Luo X, Li W, Zhong J, Cao J, Zhu S, Chen X, Zhou R, Shang C, Chen Y. TNF-α is a potential therapeutic target to overcome sorafenib resistance in hepatocellular carcinoma. EBioMedicine 2019;40:446–456.
36. Meng X, Zhu D, Yang S, Wang X, Xiong Z, Zhang Y, Brachova P, Leslie KK. Cytoplasmic Metadherin (MTDH) provides survival advantage under conditions of stress by acting as RNA-binding protein. J Biol Chem 2012; 287:4485–4491.
37. Hsu JC, Reid DW, Hoffman AM, Sarkar D, Nicchitta CV. Oncoprotein AEG-1 is an endoplasmic reticulum RNA-binding protein whose interactome is enriched in organelle resident protein-encoding mRNAs. RNA 2018; 24:688–703.
38. Luo EC, Nathanson JL, Tan FE, Schwartz JL, Schmok JC, Shankar A. Large-scale tethered function assays identify factors that regulate mRNA stability and translation. Nat Struct Mol Biol 2020;27:989–1000.
39. Wang K, Lim HY, Shi S, Lee J, Deng S, Xie T, Zhu Z, Wang Y, Pocalyko D, Yang WJ, Rejto PA, Mao M, Park CK, Xu J. Genomic landscape of copy number aberrations enables the identification of oncogenic drivers in hepatocellular carcinoma. Hepatology 2013; 58:706–717.
40. Llovet JM, Montal R, Sia D, Finn RS. Molecular therapies and precision medicine for hepatocellular carcinoma. Nat Rev Clin Oncol 2018;15:599–616.
41. Cheng A-L, Hsu C, Chan SL, Choo S-P, Kudo M. Challenges of combination therapy with immune checkpoint inhibitors for hepatocellular carcinoma. J Hepatol 2020; 72:307–319.
42. Xu J, Lin H, Li G, Sun Y, Chen J, Shi L, Cai X, Chang C. The miR-367-3p increases sorafenib chemotherapy efficacy to suppress hepatocellular carcinoma metastasis through altering the androgen receptor signals. EBioMedicine 2016;12:55–67.
43. Xu J, Lin H, Li G, Sun Y, Shi L, Ma W-L, Chen J, Cai X, Chang C. Sorafenib with ASC-J9(®) synergistically suppresses the HCC progression via altering the pSTAT3-CCL2/Bcl2 signals. Int J Cancer 2017;140:705–717.
44. Xu J, Wan Z, Tang M, Lin Z, Jiang S, Ji L, Gorshkov K, Mao Q, Xia S, Cen D, Zheng J, Liang X, Cai X. N(6)-

methyladenosine-modified CircRNA-SORE sustains sorafenib resistance in hepatocellular carcinoma by regulating β-catenin signaling. Mol Cancer 2020;19:163.
45. Xu J, Ji L, Liang Y, Wan Z, Zheng W, Song X, Gorshkov K, Sun Q, Lin H, Zheng X, Chen J, Jin RA, Liang X, Cai X. CircRNA-SORE mediates sorafenib resistance in hepatocellular carcinoma by stabilizing YBX1. Signal Transduct Target Ther 2020;5:298.
46. Lambert AW, Weinberg RA. Linking EMT programmes to normal and neoplastic epithelial stem cells. Nat Rev Cancer 2021.
47. Aiello NM, Maddipati R, Norgard RJ, Balli D, Li J, Yuan S, Yamazoe T, Black T, Sahmoud A, Furth EE, Bar-Sagi D, Stanger BZ. EMT subtype influences epithelial plasticity and mode of cell migration. Dev Cell 2018;45:681–695.e4.
48. Puram SV, Tirosh I, Parikh AS, Patel AP, Yizhak K, Gillespie S, Rodman C, Luo CL, Mroz EA, Emerick KS, Deschler DG, Varvares MA, Mylvaganam R, Rozenblatt-Rosen O, Rocco JW, Faquin WC, Lin DT, Regev A, Bernstein BE. Single-cell transcriptomic analysis of primary and metastatic tumor ecosystems in head and neck cancer. Cell 2017;171:1611–1624.e24.
49. Ye X, Tam WL, Shibue T, Kaygusuz Y, Reinhardt F, Ng Eaton E, Weinberg RA. Distinct EMT programs control normal mammary stem cells and tumour-initiating cells. Nature 2015;525:256–260.
50. Singh A, Sweeney Michael F, Yu M, Burger A, Greninger P, Benes C, Haber Daniel A, Settleman J. TAK1 inhibition promotes apoptosis in KRAS-dependent colon cancers. Cell 2012;148:639–650.
51. Bang D, Wilson W, Ryan M, Yeh JJ, Baldwin AS. GSK-3α promotes oncogenic KRAS function in pancreatic cancer via TAK1–TAB stabilization and regulation of noncanonical NF-κB. Cancer Discovery 2013;3:690–703.
52. Siegel RL, Jemal A, Wender RC, Gansler T, Ma J, Brawley OW. An assessment of progress in cancer control. CA: Cancer J Clin 2018;68:329–339.
53. An S, Zhao L-P, Shen L-J, Wang S, Zhang K, Qi Y, Zheng J, Zhang X-J, Zhu X-Y, Bao R, Yang L, Lu Y-X, She Z-G, Tang Y-D. USP18 protects against hepatic steatosis and insulin resistance through its deubiquitinating activity. Hepatology 2017;66:1866–1884.
54. Wang S, Yan ZZ, Yang X, An S, Zhang K, Qi Y, Zheng J, Ji YX, Wang PX, Fang C, Zhu XY, Shen LJ, Yan FJ, Bao R, Tian S, She ZG, Tang YD. Hepatocyte DUSP14 maintains metabolic homeostasis and suppresses inflammation in the liver. Hepatology 2018;67:1320–1338.
55. Tan S, Zhao J, Sun Z, Cao S, Niu K, Zhong Y, Wang H, Shi L, Pan H, Hu J, Qian L, Liu N, Yuan J. Hepatocyte-specific TAK1 deficiency drives RIPK1 kinase-dependent inflammation to promote liver fibrosis and hepatocellular carcinoma. Proc Natl Acad Sci U S A 2020;117:14231–14242.
56. Takezawa K, Okamoto I, Yonesaka K, Hatashita E, Yamada Y, Fukuoka M, Nakagawa K. Sorafenib inhibits non-small cell lung cancer cell growth by targeting B-RAF in KRAS wild-type cells and C-RAF in KRAS mutant cells. Cancer Res 2009;69:6515–6521.
57. Zimmerman EI, Gibson AA, Hu S, Vasilyeva A, Orwick SJ, Du G, Mascara GP, Ong SS, Chen T, Vogel P, Inaba H, Maitland ML, Sparreboom A, Baker SD. Multikinase inhibitors induce cutaneous toxicity through OAT6-mediated uptake and MAP3K7-driven cell death. Cancer Res 2016;76:117–126.
58. Wang P-X, Zhang X-J, Luo P, Jiang X, Zhang P, Guo J, Zhao G-N, Zhu X, Zhang Y, Yang S, Li H. Hepatocyte TRAF3 promotes liver steatosis and systemic insulin resistance through targeting TAK1-dependent signalling. Nature Communications 2016;7:10592.
59. Yan L, Lin M, Pan S, Assaraf YG, Wang ZW, Zhu X. Emerging roles of F-box proteins in cancer drug resistance. Drug Resist Updat 2020;49:100673.
60. Minoda Y, Sakurai H, Kobayashi T, Yoshimura A, Takaesu G. An F-box protein, FBXW5, negatively regulates TAK1 MAP3K in the IL-1beta signaling pathway. Biochem Biophys Res Commun 2009;381:412–417.

Received November 3, 2020. Accepted April 27, 2021.

Correspondence
Address correspondence to: Junjie Xu, MD, PhD, Sir Run-Run Shaw Hospital, Zhejiang University, 3 East Qingchun Road, Hangzhou 310016, Zhejiang Province, China. e-mail: walter235@zju.edu.cn; or Xiujun Cai, MD, PhD, Sir Run-Run Shaw Hospital, Zhejiang University, 3 East Qingchun Road, Hangzhou 310016, Zhejiang Province, China. e-mail: srrsh_cxj@zju.edu.cn.

Acknowledgments
The authors thank Prof Yin Sun at University of Rochester Medical Centre for experimental skills and instrumental help; Dr Lidan Hou at Zhejiang University for providing plasmids (PXF6F and PXF4H) and other reagents and instrumental help; and Dr Hui Liu at Sir Run Run Shaw Hospital, Zhejiang University School of Medicine for her professional advice on statistical analysis.

CRediT Authorship Contributions
Shunjie Xia, PhD (Conceptualization: Lead; Data curation: Lead; Software: Lead; Validation: Equal; Visualization: Lead; Writing – original draft: Lead; Writing – review & editing: Lead)
Lin Ji, PhD (Writing – review & editing: Supporting)
Liye Tao (Data curation: Supporting; Methodology: Supporting; Writing – original draft: Supporting; Writing – review & editing: Supporting)
Yu Pan, PhD (Conceptualization: Supporting; Data curation: Supporting; Methodology: Supporting; Software: Supporting; Writing – review & editing: Supporting)
Zhongjie Lin, PhD (Data curation: Supporting; Methodology: Supporting)
Zhe Wan, PhD (Writing – review & editing: Supporting)
Haoqi Pan (Methodology: Supporting; Writing – review & editing: Supporting)
Jie Zhao, PhD (Funding acquisition: Supporting)
Liuxin Cai, PhD (Funding acquisition: Supporting)
Junjie Xu, PhD (Funding acquisition: Equal; Supervision: Equal; Validation: Equal; Visualization: Supporting; Writing – original draft: Supporting; Writing – review & editing: Equal)
Xiujun Cai, MD, PhD (Funding acquisition: Lead; Validation: Lead; Writing – review & editing: Equal)

Conflicts of interest
The authors disclose no conflicts.

Funding
Supported by National Natural Science Foundation of China under grant no. 81827804 and no. 81772546 (X. Cai) and no. 81902367 (J. Xu); Zhejiang Provincial Natural Science Foundation of China under grant no. LQ18H160010 (J. Zhao) and no. LY15H160014 (L. Cai); China Postdoctoral Science Foundation under grant no. 2020M671755 (J. Xu); Hepatobiliary and Pancreatic Cancer Research of Hubei Chen Xiaoping Science and Technology Development Foundation under grant no. CXPJJH11900001-2019308 (J. Xu); Zhejiang Clinical Research Center of Minimally Invasive Diagnosis and Treatment of Abdominal Diseases grant no. 2018E50003 (X. Cai); Key Research and Development Project of Zhejiang Province under grant no. 2018C03083 (X. Cai); and Health Innovation Talent Support Project of Zhejiang Medical and Health Science and Technology Plan under grant no. 2021447581 (J. Xu).